Technical Document **2978**
August 1997

Excess System Power Available for Short-Range High-Frequency Communication Systems

D. B. Sailors

Approved for public release; distribution is unlimited.

Naval Command, Control and Ocean Surveillance Center
RDT&E Division, San Diego, CA 92152–5001

NAVAL COMMAND, CONTROL AND OCEAN SURVEILLANCE CENTER
RDT&E DIVISION
San Diego, California 92152–5001

H. A. WILLIAMS, CAPT, USN
Commanding Officer

R. C. KOLB
Executive Director

ADMINISTRATIVE INFORMATION

The work detailed in this report was performed for the Space and Naval Warfare Systems Command by the Naval Command, Control and Ocean Surveillance Center RDT&E Division, Ionospheric Branch, Code D882.

Released by
J. A. Ferguson, Head
Ionosheric Branch

Under authority of
J. H. Richter, Head
Propagation Division

SB

EXECUTIVE SUMMARY

INTRODUCTION

The Navy has used the high-frequency (HF) portion of the radio spectrum (2 to 30 MHz) for voice and low-rate data communications at ranges of from line of sight to several thousand miles. The Navy discontinued routine use of HF radio for long-range communications, but uses it intensively for inter-ship communications at ranges up to several hundred miles. At these ranges, the surface-wave mode of propagation (vice the sky-wave refraction mode) can provide good communications performance around the clock with proper frequency and antenna selection. Since the HF surface wave does not have the multiple path and fading problems associated with HF sky-wave refraction, it is said to be "non-dispersive" and regularly provides a higher quality channel. Therefore, it can potentially support channels of much greater bandwidth than those normally used for HF communications.

In 1995, experiments conducted by the Naval Command, Control and Ocean Surveillance Center RDT&E Division (NRaD) over a 65-mile path over seawater easily supported data rates of 56 kbps within a 40-kHz bandwidth. As a result of these experiments the Office of Naval Research (ONR) funded a proposal with a goal of providing up to 128 kbps in a 40-kHz signal bandwidth.

This report presents the results of a surface-wave propagation study with a goal to relate transmission power to expected range and received signal-to-noise ratio (SNR). Results are normalized to a 1-Hz bandwidth that permits path estimates for both conventional narrowband signals as well as extension to wideband signals.

OBJECTIVE

The study's objective was to determine the excess available transmission power over sea for a short-range (i.e., less than 500 km), high-frequency (HF) communication system.

RESULTS

The sensitivity of the required radiated power was analyzed for ship-to-ship, short-range HF communications for all the various variables affecting the link. The excess transmission power over that required for link operation was determined and displayed for the different input parameters affecting its performance. Engineers calculated the excess available transmission power using a computer program developed for this purpose called the Point-to-Point Propagation (PTPP) program. This program utilizes the SRI International AMBCOM programs NATGEN and RAYTRA for its ionospheric path calculations, an Institute for Telecommunications Sciences program GW for its ground-wave path signal strength or basic transmission-loss calculations for elevated antennas over a smooth spherical earth, and a program, REL2, for the combination of the signal strengths of the ionospheric modes and ground-wave mode and for the determination of the excess available transmission power. The program produces an output file similar to an IONCAP Method 23 output.

The excess transmission power was calculated as a function of time of day, position in the solar cycle given by the sunspot number, and season, for a required system SNR of 45 dB in a 1-Hz receiver noise bandwidth, 0-dB antenna gains, and 1,000 watts of transmitted power, and the

mode of propagation (sky wave and the combination of both ground-wave and sky-wave modes). The results are divided into (1) high radio noise location; (2) median radio noise location; (3) low radio noise location; (4) high-latitude location; (5) sky-wave only; and (6) the affects of system time availability.

The high radio noise location had the least amount of excess power available of all four radio noise locations considered. As was the case for all the receiver locations, the available excess power decreases with increasing frequency and range. At some combinations of these parameters, especially at the higher frequencies and ranges, no excess power is available. At midnight in January there is a decrease in available excess power over that at local noontime. However, at midnight there is little difference in the variation in the excess available power as a function of sunspot number. For the month of July, there is a decrease in available excess power at the lowest frequencies at local noontime compared to that in January. In July as in the January case, there is a decrease in the available excess power at midnight compared to local noontime. In the July case at local midnight at a range of 500 km, however, there is not sufficient power at low sunspot numbers to meet the system requirements. However, at the higher sunspot numbers 110 and 160, there is excess available power at a single frequency due to the presence of a sky-wave mode. For July, sunspot number 160, and local midnight; the excess power at the optimum frequency is approximately 40 dB, 26 dB, 15 dB, 8 dB, and 2 dB at the ranges 100 km, 200 km, 300 km, 400 km, and 500 km, respectively. At the high-latitude radio noise location, the results were entirely influenced by the ground-wave mode of propagation and, thus, auroral absorption effects are of no concern for path ranges considered and were not displayed.

For the conditions of sunspot number 160 and July at the high radio noise receiver location, the sky-wave mode only calculations show that only a narrow range of frequencies at only a few ranges exhibit any excess available power because of the high take-off angles for near-vertical incidence systems.

The required system time availability calculations show that: (1) there is a greater excess of available power for each range at 75% than at 95% time availability; (2) local noon peaks at lower frequencies than does local midnight; and (3) as the range is increased, the difference in excess power between 75% and 95% time availability decreases considerably.

Three additional topics were discussed. First, a table of required SNRs for various HF systems is given. As can be seen from the table, some HF systems have a much larger required SNR than 45 dB in a 1-Hz receiver noise bandwidth (i.e., equivalent to 10.2 dB in a 3-kHz receiver noise bandwidth). These types of systems would be operable only at the lower HF frequencies and shorter ranges. For reference purposes, advanced narrowband secure voice terminal (ANDVT) has a required SNR value of 41.8 dB in a 1-Hz receiver noise bandwidth (i.e., 7 dB in a 3-kHz receiver noise bandwidth), and DPSK Link–11 has a required SNR of 62.8 dB in a 1-Hz receiver noise bandwidth in the presence of atmospheric noise and Rayleigh-fading (i.e., 25 dB in a 6-kHz receiver noise bandwidth). As a tentative point of reference for HF wideband operation, experiments with a QPSK waveform at 64 kbps showed that a SNR value of 62 dB in a 1-Hz receiver noise bandwidth (i.e., Eb/No of 14 dB) yielded near error-free operation. Second, the antenna gain for surface-wave transmission is discussed; two vertical half-wave dipoles at ground level would raise the excess power curves by only 4.3 dB. For shipboard antennas, the antenna is lossy and has an average gain over all frequencies and take-off angles measured of -9.65 dB, and there

is a necessary added protection factor of 7.5 dB for 90% coverage necessary to account for the uncertainty of directional characteristics of the shipboard antennas. Thus, for lossy shipboard antennas there is a net adjustment downwards of -11.13 dB that includes a 6.02-dB adjustment in the system transmission loss for surface-wave propagation for antennas one-half wavelength above the ground. Finally, the added transmission loss caused by rough seas, calculated using a representation of Barrick's rough earth surface impedance model in appendix A, is plotted versus frequency for each of the five ranges in the study for six different sea states. The affect of sea state peaks at different ranges and frequencies than it does at the frequencies for optimum short-range communications. The actual impact depends on the communication frequencies used. Further, sea states with higher wind speeds take longer to become fully arisen than those with the lower sea states and would not be encountered often in practice.

RECOMMENDATIONS

1. Consider the surface-wave mode of propagation over the sea at HF frequencies as a viable mode out to 500 km.
2. Consider the possibility that the surface-wave mode of propagation over the sea at HF frequencies might be usable out to 1,000 km.
3. Utilize tables such as table 1 and table 2 for a source for values of required SNR in a 1-Hz receiver noise bandwidth if measured values for a particular system are not available.
4. In determining the affects of sea state on surface-wave mode of propagation over the sea, consider only the sea states 1 through 4.
5. Utilize the rough earth surface impedance model in appendix A in a surface-wave computer program to calculate the affects of sea state on surface-wave propagation.
6. Use mixed path calculations for surface-wave propagation to include sea state only on that portion of the path for which it applies.

CONTENTS

FIGURES

TABLES

INTRODUCTION

This report analyzes the required radiated power sensitivity for ship-to-ship, short-range, high-frequency (HF) communications to all the various variables that could affect the link. The Naval Command, Control and Ocean Surveillance Center RDT&E Division (NRaD), Ionosheric Branch, Code D882, determined the excess transmission power for the different input parameters affecting its performance over that required for link operation. The excess available transmission power was calculated as a time-of-day function, position in the solar cycle, season, required system signal-to-noise ratio (SNR) and time availability, and propagation mode (i.e., sky wave, ground wave, or the combination of both). This choice of calculation variables was based on a basic HF communication system link analysis conducted by Olson (1983), which determined some of the various parameters that could affect link performance.

This report is organized as follows. First, the report presents a description of the analysis approach. Second, it provides a background on the computer program used for the analysis. Third, the RESULTS section includes the following subsections:

1. High radio noise location
2. Median radio noise location
3. Low radio noise location
4. High-latitude receiver location
5. Sky-wave propagation only
6. Affects of system time availability

Fourth, the DISCUSSION section reviews some important considerations, namely, the factors most affecting the available excess transmission power:

1. Radio noise level at the receiver location
2. System required time availability
3. Antenna gain
4. Effects of sea roughness on the surface-wave propagation

Finally, appendix A discusses the surface impedance model added to the ground-wave computer program. The model was used to produce the results presented concerning the affects of sea roughness on the surface-wave propagation. Appendix B provides verification data concerning the accuracy of the surface impedance model of appendix A.

APPROACH

The Coverage Propagation Prediction (CPP) program, a propagation program that computes excess system power for both ground-wave propagation and sky-wave propagation modes, was used as a starting point for the analysis results discussed in this document. The program was modified to predict the propagation on a point-to-point propagation path. This entailed:

1. Increasing the maximum number of possible input frequencies to that allowed by one of its component programs, AMBCOM.
2. Removing multiple receiver site parameter information input.
3. Adding options for allowing the calculation of either sky-wave propagation modes or ground-wave modes without the presence of the other.
4. Rewriting output files to allow them to be read by a graphics plotting program.
5. Adding an option to use the original International Radio Consultative Committee (CCIR) Report 322 atmospheric radio noise model for receiver locations where the current CCIR Report 322-3 atmospheric radio noise model has a serious discrepancy (Sailors, 1995).
6. Adding a constant gain antenna pattern.
7. Adding an antenna pattern with constant gain plus 10 LOG (COS Δ) where Δ is the take-off angle.
8. Modifying the input to allow for incrementing the environmental variables effecting the calculated results.
9. Removing specific input parameters written into the source code that were required by the specific Navy system for which the CPP program was originally designed.
10. Modifying the output so that an output similar to that of a commonly used HF propagation prediction program, IONCAP, could be produced.

The resulting program is called the Point-to-Point Propagation (PTPP) program. Figure 1 presents a flow chart of the overall flow of the PTPP program. Four separate programs are called. These are the programs DATIN, NATGEN, RAYTRA, and REL2.

First, PTPP calls the program DATIN to load all the input parameters for the computation. This includes loading the system parameters, the K_p index used for auroral absorption calculations, the range of times of day, of months, of sunspot numbers, and up to 24 frequencies. Then files that have the transmitter locations and receiver locations for the computations are either created or loaded by DATIN. The transmitter location can be either a single location or locations on a radial out from the receiver location. The transmitter data include the transmitter antenna bearing information. The receiver location file includes data unique to each receiver location. (Note that for point-to-point computation only one receiver location is assumed.) Antenna types for each transmitter location and receiver location are determined from a list of 10 choices, or read from the input files if they exist. The receiver location data file, if it exists, contains the receiver bearing, the man-made noise environment, the ground distance over land at the receiver site (a value of zero indicates ship-to-ship), and the choice of CCIR atmospheric noise model. The Program options that are loaded by DATIN include the choice of HF propagation model or models (i.e., sky-wave and/or ground-wave models) and, for sky-wave propagation, a choice as to whether the path is a near-vertical incidence path or a normal HF system. The

propagation model choices include sky-wave propagation only, ground-wave propagation only, or both sky-wave and ground-wave propagation.

Once DATIN inputs all the data, an output file called "datinput" is created for use by PTPP, and control is returned to PTPP.

Within PTPP there are three major loops. These loops are, in turn, a month loop, a sunspot loop, and a transmitter location loop. Input provided by DATIN determines the beginning, ending, and incrementing values. Within these loops three programs (NATGEN, RAYTRA, and REL2) are called, in turn, for every path in the analysis (e.g., for five transmitters on a radial to a receiver, these three programs are called, in turn, five times.). Before the loops are entered, the "DATINPUT" file is opened by PTPP, and the data are read into memory. Prior to the execution of the transmitter loop, the transmitter location file "TRMITF" is opened. Within the transmitter loop, the transmitter data are read for each transmitter location as they are processed. Three files ("NATIN," "RAYIN," and "USRIN") are opened for providing files to write data for subsequent processing by these three programs. Data required by these programs are written in these files and the files closed. Finally, output data headings for the printed output of REL2 are produced.

The first program called is NATGEN. Depending on path length, the program NATGEN determines the locations and parameters for up to 41 different ionospheric electron density profiles for the minimum Zulu time, for each time interval up to and including the maximum Zulu time input. NATGEN also includes models for representing the high-latitude ionosphere. NATGEN produces an output file (IONOS.DAT) containing the electron density profiles along the great circle path between the transmitter receiver pair.

The second program in the sequence, RAYTRA, reads the IONOS.DAT file produced by NATGEN. The RAYTRA program utilizes a homing procedure with an open-ended, semi-analytic, two-dimensional ray trace through the modeled ionospheric electron density profiles to predict signal loss and ray launch and reception angles for each propagating mode for the path. RAYTRA includes an auroral absorption model to represent the additional transmission losses occurring at high latitude. RAYTRA determines the radio noise at the receiver site using either the original or the current CCIR model, depending on an input parameter input in DATIN for each receiver site. RAYTRA produces a file (COMEFF.DAT) that contains a list of propagating modes for each frequency and receiver location. For each mode, the files contain, among other parameters, the launch angle and receive angles and the total path transmission loss. For each frequency and receiver site, this file also contains the median external noise power and the 84^{th} and 16^{th} percentiles of the noise distribution. A second file called NOISPWR.DAT is also written for use in the REL2 program when no ionospheric exists. This file contains the median noise external power and percentiles of the noise distribution at each receiver site and for each frequency.

REL2 reads the output files produced by RAYTRA (COMFF.DAT and NOISPWR.DAT) and PTPP (USRIN) to determine the circuit reliability for the each propagating mode determined by RAYTRA for each frequency on the link. When determining the mode's reliability, it is assumed that the signal and noise are statistically independent and that the distribution of signal-to-noise ratio (SNR) could be represented by a standard normal distribution. Having determined the mode's reliability for the sky-wave modes, the reliability is then determined for the ground-wave mode for path ranges out to 1000 km. With the mode's reliability determined, the circuit reliability is calculated by combining the individual mode's reliability in a manner similar to that used in IONCAP (Teters et al., 1983). Finally,

this value is used to determine the required transmitter power for a given required reliability (time availability). A positive value indicates an excess amount of transmitted power.

The processing within REL2 begins with a call to the subroutine GETANT to load the antenna gain arrays. Then the files "COMEFF.DAT," "USRIN," and "NOISPWR.DAT" are opened. Output files are opened to output data for printing and plotting. The file name depends on user input. Next, a time loop begins running from the minimum time up to and including the last Zulu time. Within this loop the subroutine GWREL2 is called to determine the reliability of the ground-wave mode. The subroutine GWREL2 calls the subroutine GW. The subroutine GW is a ground-wave program developed by Leslie Berry at the Institute for Telecommunications Sciences for calculation of the ground-wave signal strength or basic transmission loss for elevated antennas over smooth, spherical earth (Berry, 1978). The subroutine OUT creates the final print file. This output file is similar to an IONCAP Method 23 output. For each frequency, the SNR, the excess power, and the reliability are output. This ends the time loop. The output files are closed.

Control returns to PTPP once the link analysis is completed. The analysis repeats for additional links, sunspot numbers, and months, if any exist.

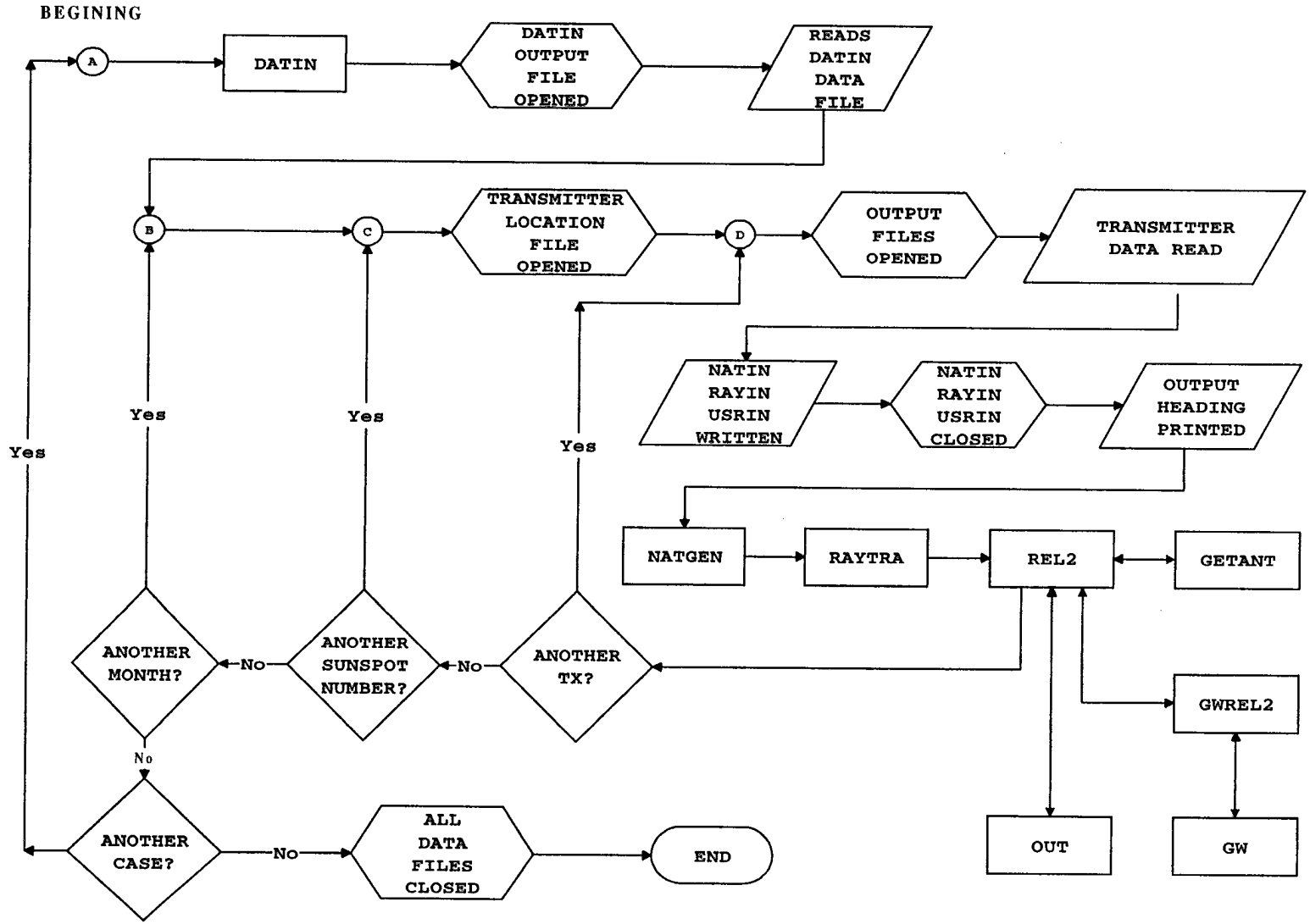

Figure 1. Flowchart for the Point-to-Point Propagation (PTPP) program.

BACKGROUND

The Coverage Propagation Prediction (CPP) Program is a high-frequency (HF) propagation prediction tool designed at NRaD to analyze the transmission coverage provided by multiple receiver sites for a particular Navy communication system. It includes both sky-wave and ground-wave propagation modes. The inclusion of the ground wave is important because when the intended receiver is within the so-called sky-wave skip zone of the transmitter, the ground wave is the only mode of propagation on the path. A prediction of this mode significantly improves the area coverage prediction of short-range transmissions. The CPP program and the SPP program described below are the only programs that include the combination of both the sky-wave and ground-wave modes.

The CPP program is based on the Shipboard Propagation Prediction (SPP) Program developed for frequency selection by the same Navy communication system (Sprague, 1993a and 1993b). It uses the AMBCOM prediction program as an integral part (Hatfield et al., 1987; Smith and Hatfield, 1987). In the SPP program, the capability to calculate circuit reliability was added to the AMBCOM capability of calculating the signal-to-noise ratio (SNR) on a propagation path. For each of the intended receiver sites, the SPP program predicts the circuit reliability at five frequencies for a given transmitter location, time of day, month, and sunspot number.

The CPP program predicts an additional parameter not calculated in the SPP program. This parameter is the required power margin for a required reliability (e.g., 90%). For the required reliability (required time availability), the power margin is the difference in dB between the available SNR for the required system SNR for the grade of service required by the communication system. It accounts for the day-to-day variability in both the signal strength and noise power. A positive value indicates an excess of available transmitted power. The excess available transmitted power allows one to determine the effects of both different antenna systems from the peak gains and different communication systems from the required SNRs. This does not require the recalculation of the propagation transmission loss and radio noise.

In both of these programs, CPP and SPP, the median ground-wave transmission loss is predicted by the GW87PC program developed by Berry (1978). Millington's method for calculating field strength over inhomogeneous earth is used to allow for ground-sea transitions (Millington, 1949). These values of transmission loss are combined with system-specific operational parameters (transmitter power, path antenna gain) to obtain the mode received power. When combined with the medium noise power as predicted by AMBCOM, the median signal noise is obtained for each mode (ground wave and sky wave).

A second program, FILCONV, processes the large volume of output data from the CPP program. Another program, DATIN, determines the transmitter locations for use with CPP in an operating area given the boundary defining the area and creates the files containing the arcs of antenna coverage to be used in the coverage analysis.

The programs CPP, DATIN, and FILCONV are written in the FORTRAN programming language.

RESULTS

The PTPP program was run for several combinations of possible input variables to determine the significant variables controlling the required transmission power. The variables considered are those suggested by Olson (1983). These include the path range, the solar condition given by the sunspot number, the season represented by the month, the time of day, the K_p index used for the auroral absorption calculations, the location of the receiver site based on its probable radio noise level, and the required reliability (time availability). The fixed parameters include the frequencies, the required signal-to-noise ratio (SNR), the transmitter power, the antenna gain, and the man-made noise environment. Two other variables were program options to choose the atmospheric radio noise model for each receiver location and to choose whether ground-wave or sky-wave were calculated by themselves or combined together. No calculations were performed for ground-wave propagation by itself. Sky-wave only calculations were made only for sunspot number 160 and the month of July, representing summer. All sky-wave calculations were made assuming a near-vertical incidence system (NVIS). For a NVIS, the ray tracing for the sky-wave modes is for the take-off angles of 40 to 85 degrees.

Figure 2 shows a sample of a prediction by the PTPP program for one set of input parameters. The figure shows the path range in km, the bearing at the receiver towards the transmitter, the bearing at the transmitter towards the receiver, the antenna azimuths if any (zero is used for an omni-directional antenna), values of constant gain input for the transmitter and receiver antennas, the ground distance over land at the receiver site (a value of zero for ground distance [GDIST] indicates ship-to-ship), the antenna gain patterns chosen, and the fixed and variable parameters used for the calculations. The fixed variables actually used include: (1) 1,000 watts of transmitted power; (2) 45-dB required SNR in a 1-Hz receiver noise bandwidth (i.e., equivalent to 10.2 dB in a 3-kHz bandwidth); (3) 0-dB antenna gains; (4) ship-to-ship communications (i.e., the value of the GDIST is 0.0); (5) a rural man-made noise environment; and (6) 90% required reliability for all the calculations except those noted below. The figure shows three sets of lines for calculated results. Each set of lines is for eight input transmission frequencies. The 24 frequencies used in the calculations were 2, 3, 4, 5, 6, 7, 8, 9, 10, 11, 12, 13, 14, 15, 16, 17, 18, 19, 20, 22, 24, 26, 28, and 30 MHz, which were used for all calculations. The parameters given in these lines are the time of day, the frequencies used, the SNR dB, the required power margin (REQ POW MARGIN dB)—the excess power, and the reliability (REL PERCENT). A value of -99.0 for the required power margin indicates that no mode of propagation was available for the frequency.

Variable parameter values used in the calculations are as follows. First, four types of receiver locations were chosen representing the level of radio noise likely to be received at these receiver sites. These areas represent high-noise areas, medium-noise areas, low-noise areas, and high-latitude areas. The coordinates used for these four locations, respectively, were (13°N, 112°E), (27°N, 136°E), (34°N, 20°E), and (60°N, 30°W). For the last location, normal ionospheric propagation was considered as well as an ionospheric storm given by using K_p equals 6 instead of the median value of 3. Also, at this location the original CCIR atmospheric noise model was used as recommended by Sailors (1995) rather than the current model. Second, calculations were made in an easterly direction from the receiver locations at ranges of 100, 200, 300, 400, and 500 km at local noon and midnight at each of these locations. Third, calculations were made at sunspot numbers of 10, 60, 110, and 160 and for the months of

January, April, July, and October. Finally, at the high-noise receiver location for July and sunspot number 160, calculations were conducted for values of time availability of 75%, 80%, 85%, 90%, and 95% to see the effect a varying user requirement for high performance.

```
POINT-TO-POINT PROPAGATION PROGRAM                    22 APR 1996
         JUL   1996  SSN =  160.  FLUX =   204.  KP =    3.
high noise receiver area
  13.00 N  -112.92 W TO highn   13.00 N  -112.00 W
PL KM     99.6 AZ TO REC   270.1 AZ TO TR   89.9
T AZIMUTH     .00 R AZIMUTH   90.00 T CGAIN   .00 R CGAIN   .00 R GDIST     .00
 CONSTANT GAIN ANTENNA              CONSTANT GAIN ANTENNA
POWER    1000. MAN-MADE NOISE Rural          REQ.SNR  45.0  REQ. REL  90.0 %
Sky wave and ground wave     near vertical incidence system    CCIR 322-3 Noise

5 UT      2.0    3.0    4.0    5.0    6.0    7.0    8.0    9.0 FREQ
         95.8   97.8   98.5   98.8   98.7   98.4   98.0   97.4 SNR dB
         42.9   46.1   47.3   47.7   47.8   47.6   47.2   46.6 REQ POW MARGIN dB
        100.0  100.0  100.0  100.0  100.0  100.0  100.0  100.0 REL PERCENT


5 UT     10.0   11.0   12.0   13.0   14.0   15.0   16.0   17.0 FREQ
         96.6   95.7   94.6   93.5   92.4   91.2   90.1   89.0 SNR dB
         46.0   45.1   44.1   43.1   42.1   41.0   39.9   38.8 REQ POW MARGIN dB
        100.0  100.0  100.0  100.0  100.0  100.0  100.0  100.0 REL PERCENT


5 UT     18.0   19.0   20.0   22.0   24.0   26.0   28.0   30.0 FREQ
         88.0   86.9   86.0   84.1   82.5   80.9   79.3   77.7 SNR dB
         37.8   36.8   35.8   33.9   32.2   30.5   28.8   27.2 REQ POW MARGIN dB
        100.0  100.0  100.0  100.0  100.0  100.0  100.0  100.0 REL PERCENT
```

Figure 2. Sample Point-to-Point Program (PTPP) output showing excess power at a high-noise area for a required SNR of 45 dB, a required reliability of 90%, and a 0-dB gain, at sunspot number 160 for July (12:00 LT).

HIGH RADIO NOISE LOCATION

Figures 3 through 14 show the results of the high radio noise location. This location has the least amount of excess power available of all the four radio noise locations considered. The amount of excess power is dependent upon the sunspot number, month, time of day, path range, and frequency. Calculations conducted at all the receiver locations illustrate the available excess power decreases with increasing frequency and range. At some combinations of these parameters, no excess power is available. Each figure shows the excess power available at each frequency for a required SNR in a 1-Hz receiver noise bandwidth of 45 dB, a required reliability of 90%, and 0-dB antenna gains at the ranges of 100 km, 200 km, 300 km, 400, km, and 500 km. The figures also show the excess power for the optimum frequency at each range. The optimum frequency is the highest frequency with the highest excess power (i.e., it is possible for adjacent frequencies to have the same excess power. The highest frequency is chosen as optimum).

Figures 3 through 6 show the range and frequency dependence of the excess available power for the extreme sunspot numbers 10 and 160 for the month of January at the high-noise area receiver location. Figures 3 and 4 are for sunspot number 10 for the hours 12:00 and 24:00 local time, respectively. Figures 5 and 6 are for the sunspot number 160 for the hours 12:00 and 24:00 local time. Figures 4 and 6 show that the available excess power decreases for local midnight. Figures 3 and 5 show that at midnight there is a decrease in available excess power over that at local noontime. However, at the midnight hour there is little difference in the

variation in the excess available power as a function of sunspot number. Figures 3 and 5 do show the effect of sunspot number during the local noontime. At a range of 500 km, one frequency in figure 5 shows an increase in available excess power. This is due to the presence of a strong ionospheric mode not present at other sunspot numbers and hours during the day. Generally, these results are due to propagation of the ground wave except at this one frequency, sunspot number, and time of day.

Figures 7 through 14 show the range and frequency dependence of the excess available power for the month of July for the high-noise area receiver location for four sunspot numbers. Figures 7 and 8 are for sunspot number 10 for the hours 12:00 and 24:00 local time, respectively. Figures 9 and 10 are for sunspot number 60 for the hours 12:00 and 24:00, respectively. Figures 11 and 12 are for sunspot number 110 at the hours 12:00 and 24:00, respectively. And figures 13 and 14 are, in turn, for hours 12:00 and 24:00 at sunspot number 160. Figures 7, 9, 11, and 13 show the effect of sunspot number at local noontime. For the month of July, there is a decrease in available excess power at the lowest frequencies shown for local noontime over that shown for local noontime for January in figures 3 and 5. Figures 8, 10, 12, and 14 show the effect of sunspot number at local midnight. As for the January case, there is a decrease in available excess power compared to that for local noon. In the July case at local midnight, however, at a range of 500 km, there is insufficient power to meet the requirements of 90% time availability, a 45-dB required SNR, 0-dB antenna gains, and 1,000 watts of transmitted power. However, for this case, at sunspot numbers 110 and 160, there is an increase in SNR of the sky-wave mode, causing excess available power at a single frequency. Of course this effect is most notable at the extreme sunspot number of 160; whereas, at sunspot number 110 this increase is only slight.

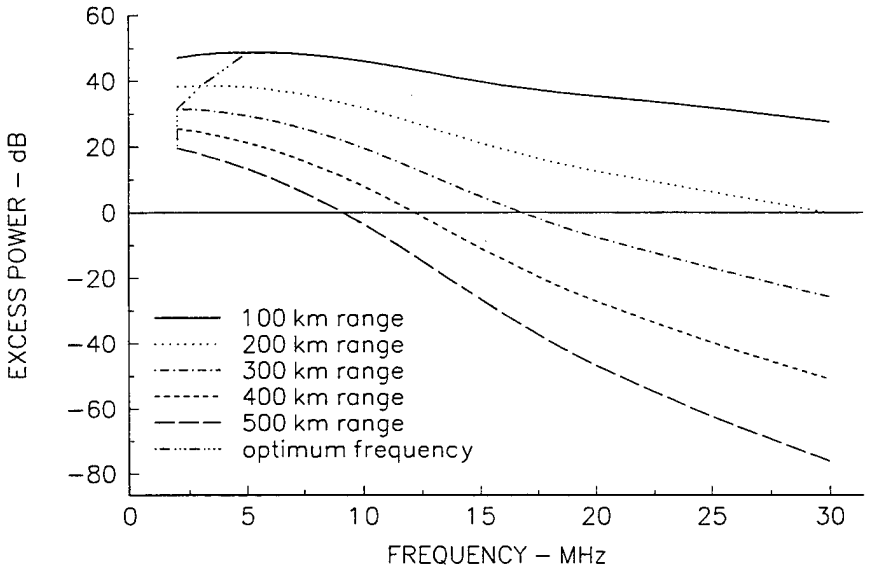

Figure 3. Excess power at a high-noise area for a required SNR of 45 dB, a required reliability of 90%, and a 0-dB antenna gain, at sunspot number 10 for January (12:00 LT).

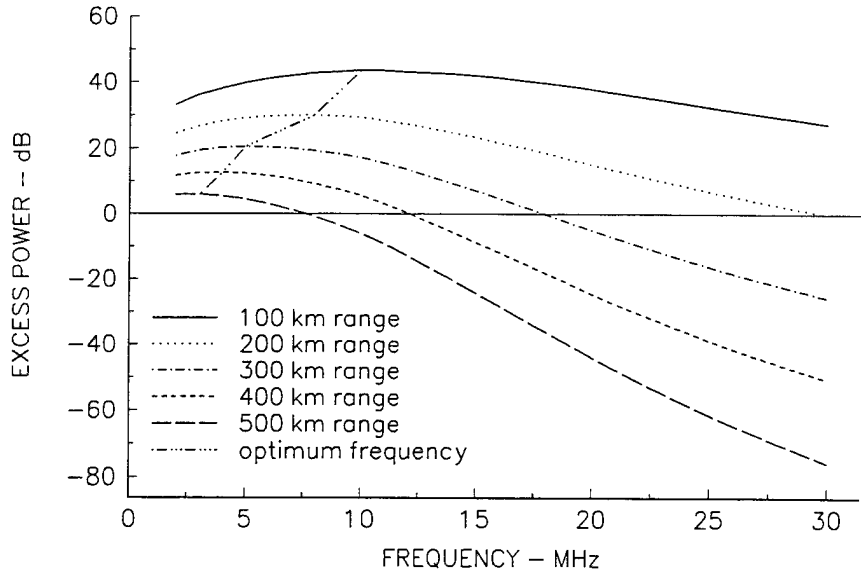

Figure 4. Excess power at an high-noise area for a required SNR of 45 dB, a required reliability of 90%, and a 0-dB antenna gain, at sunspot number 10 for January (24:00 LT).

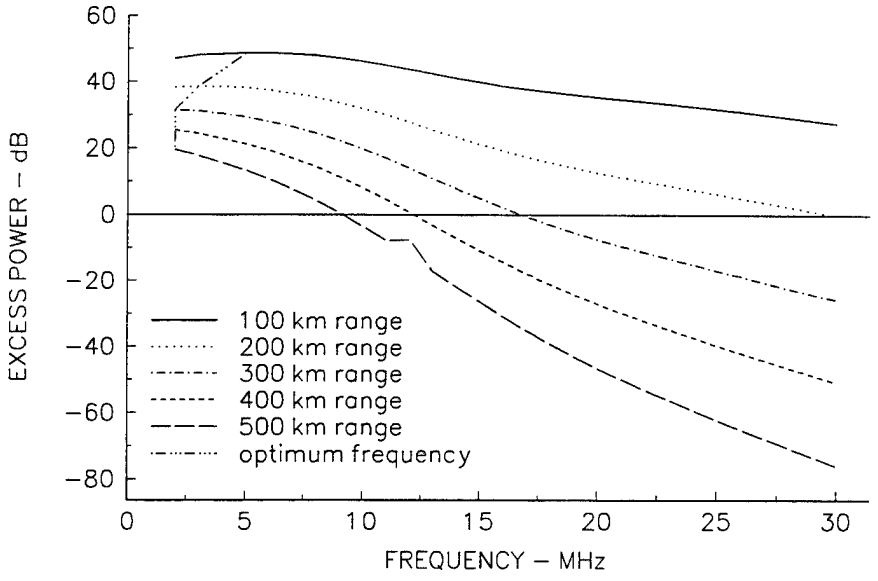

Figure 5. Excess power at a high-noise area for a required SNR of 45 dB, a required reliability of 90%, and a 0-dB antenna gain, at sunspot number 160 for January (12:00 LT).

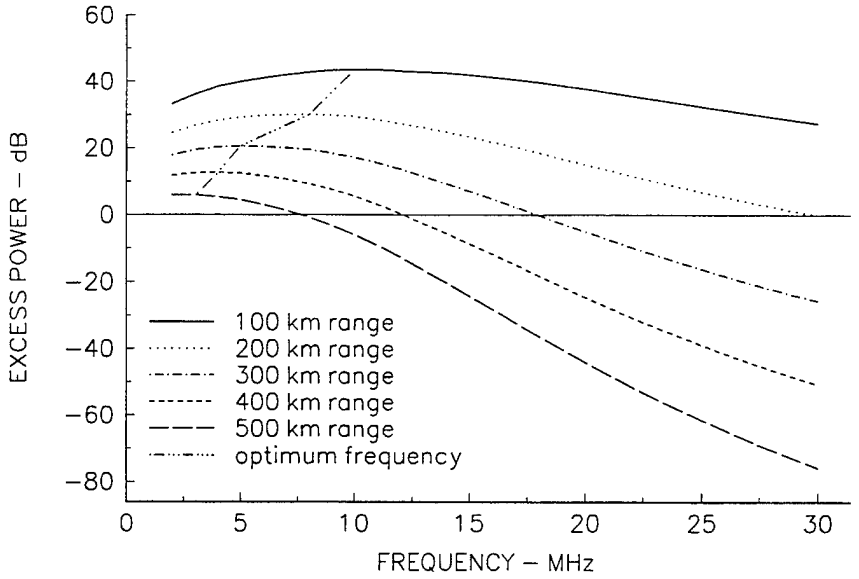

Figure 6. Excess power at a high-noise area for a required S/N ratio of 45 dB, a required reliability of 90%, and a 0-dB antenna gain, at sunspot number 160 for January (24:00 LT).

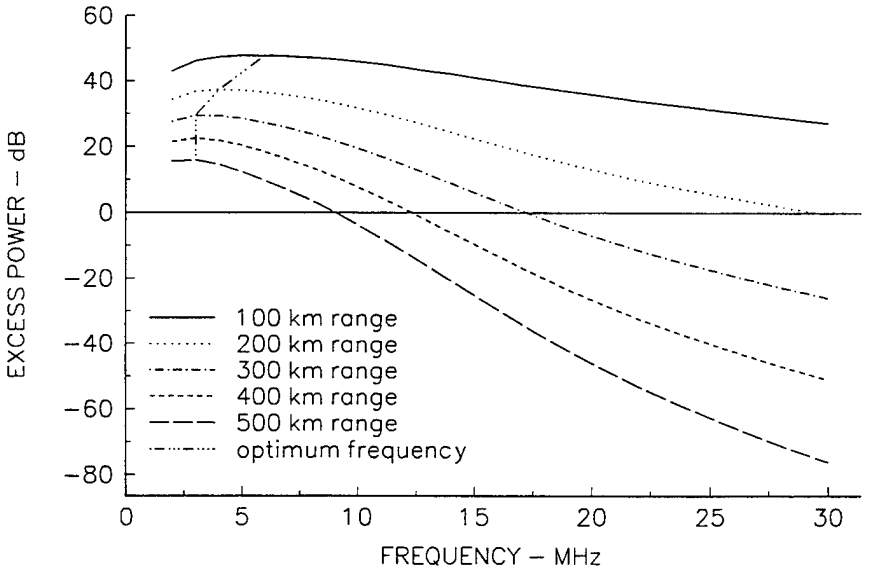

Figure 7. Excess power at a high-noise area for a required SNR of 45 dB, a required reliability of 90%, and a 0-dB antenna gain, at sunspot number 0 for July (12:00 LT).

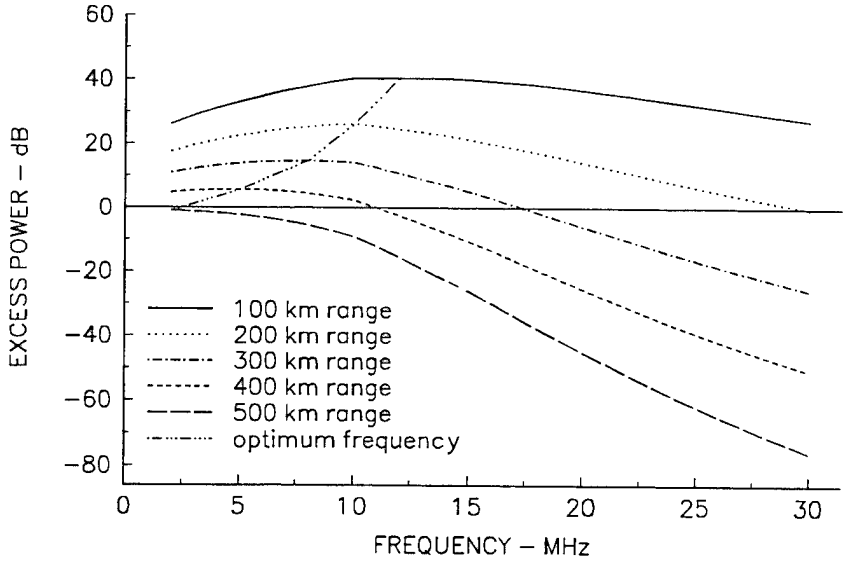

Figure 8. Excess power at a high-noise area for a required SNR of 45 dB, a required reliability of 90%, and a 0-dB antenna gain, at sunspot number 10 for July (24:00 LT).

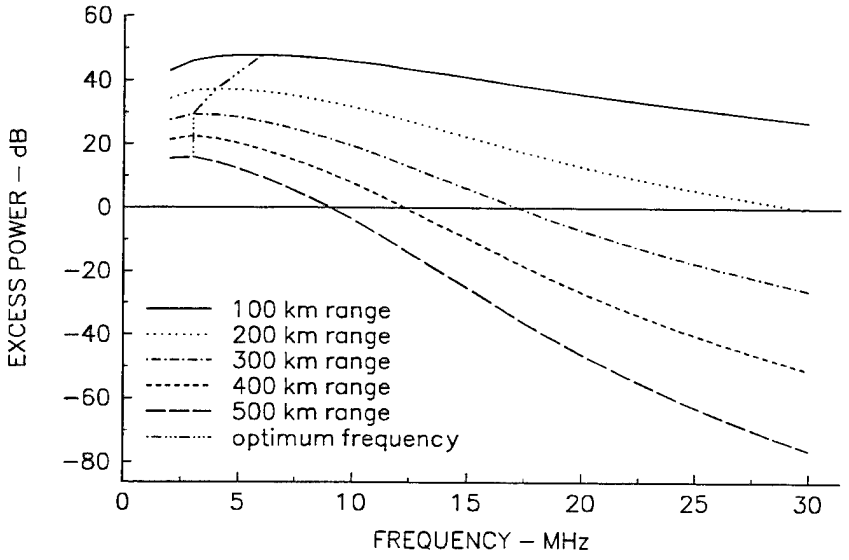

Figure 9. Excess power at a high-noise area for a required SNR of 45 dB, a required reliability of 90%, and a 0-dB antenna gain, at sunspot number 60 for July (12:00 LT).

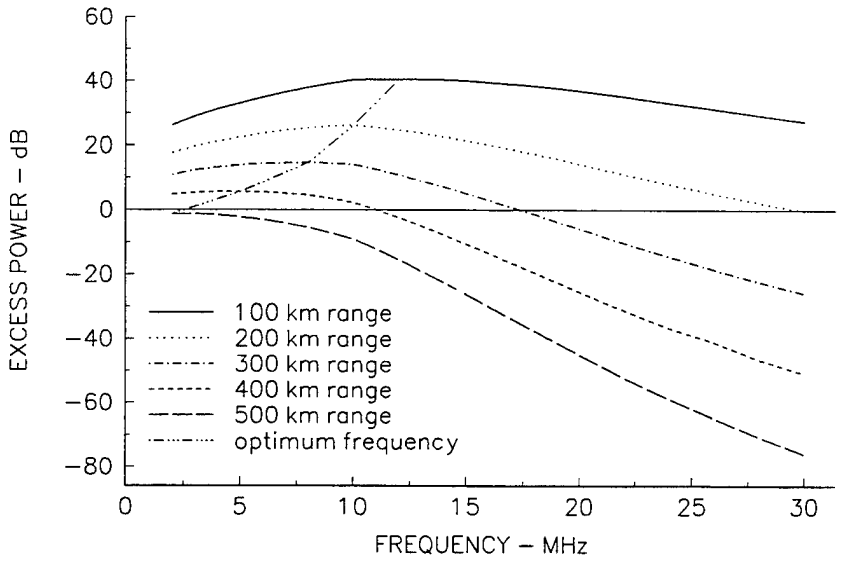

Figure 10. Excess power at a high-noise area for a required SNR ratio of 45 dB, a required reliability of 90%, and a 0-dB antenna gain, at sunspot number 60 for July (24:00 LT).

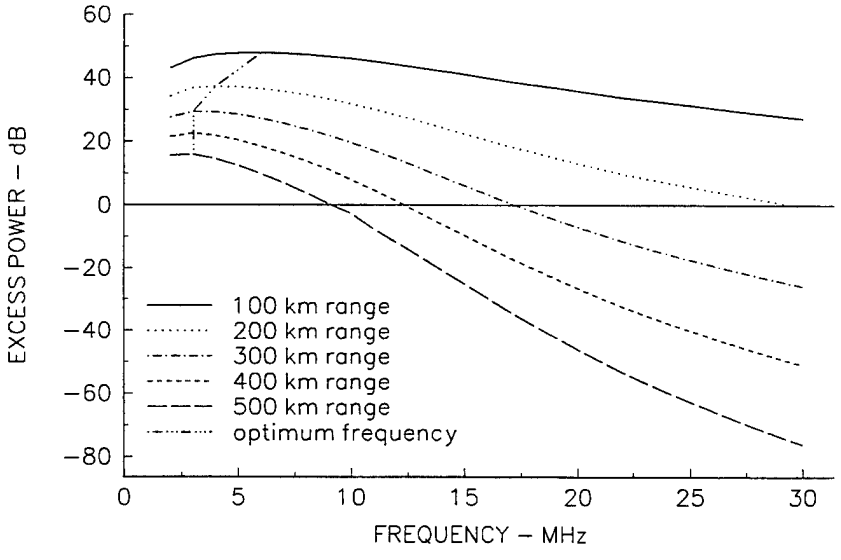

Figure 11. Excess power at a high-noise area for a required SNR ratio of 45 dB, a required reliability of 90%, and a 0-dB antenna gain, at sunspot number 110 for July (12:00 LT).

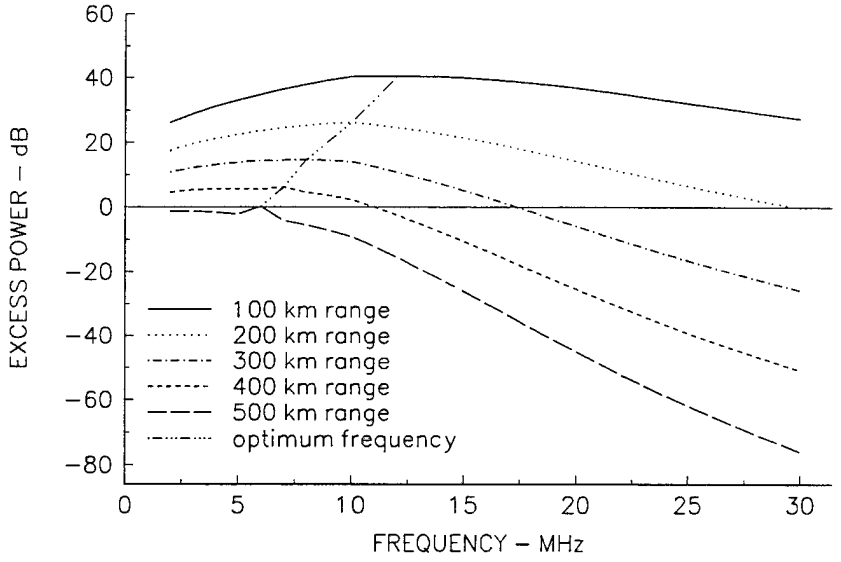

Figure 12. Excess power at a high-noise area for a required SNR ratio of 45 dB, a required reliability of 90%, and a 0-dB antenna gain, at sunspot number 110 for July (24:00 LT).

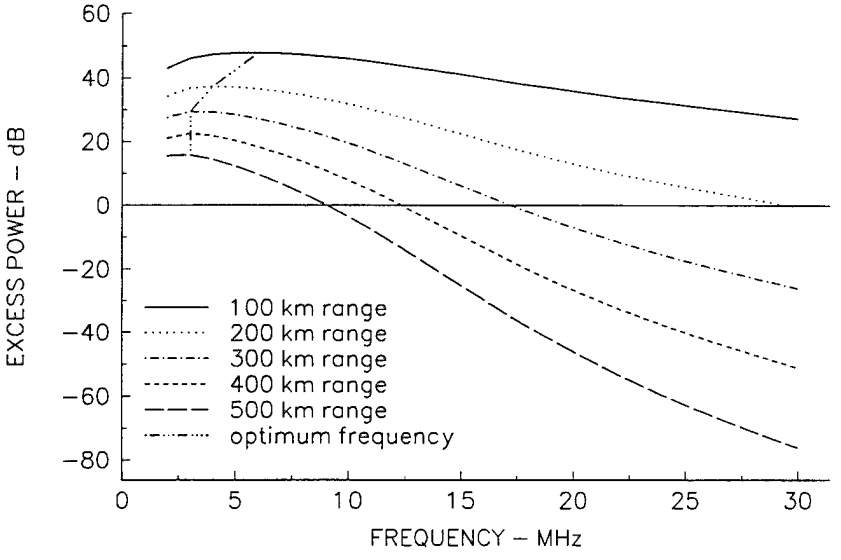

Figure 13. Excess power at a high-noise area for a required SNR ratio of 45 dB, a required reliability of 90%, and a 0-dB antenna gain, at sunspot number 160 for July (12:00 LT).

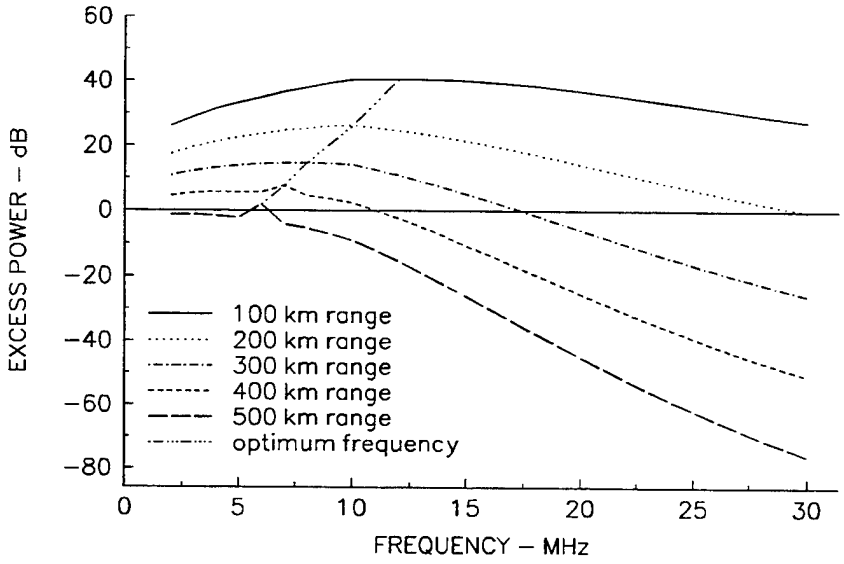

Figure 14. Excess power at a high-noise area for a required SNR of 45 dB, a required reliability of 90%, and a 0-dB antenna gain, at sunspot number 160 for July (24:00 LT).

MEDIAN RADIO NOISE LOCATION

Figures 15 through 22 show the range and frequency dependence of the excess available power for the median radio noise receiver location. Figures 15 through 18 are for the month of January. Figures 19 through 22 are for the month of July. Figures 15 and 16 are for the month of January at sunspot number 10 at the hours of 12:00 and 24:00 local time. Figures 17 and 18 are for January at sunspot number 160 at the hours of 12:00 and 24:00 local time. In the same manner, for July, figures 19 and 20 are for the hours 12:00 and 24:00, respectively, at sunspot number 10. Figures 21 and 22 are for 12:00 and 24:00 local time, respectively, at sunspot number 160. For local noontime, the controlling factor in these figures appears to be the radio noise, not the sunspot number or season. However, at local midnight the results are different. First, there is a decrease in excess available power caused by an increase in radio noise at local midnight. In addition, during January there is an apparent appearance of a strong ionospheric mode of propagation at about 12 MHz at sunspot number 160. At sunspot number 160 in July, there is a strong ionospheric mode at about 7 MHz at a range from 400 to 500 km.

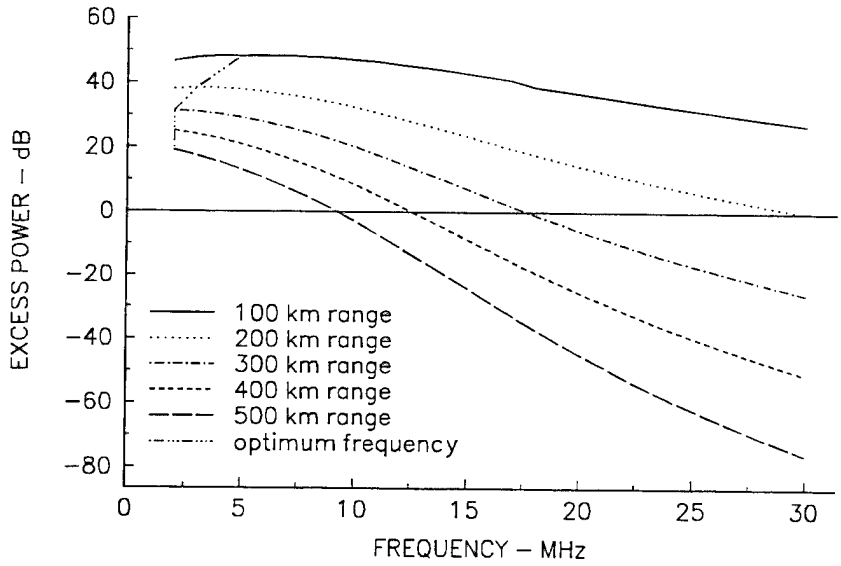

Figure 15. Excess power at a medium-noise area for a required SNR ratio of 45 dB, a required reliability of 90%, and a 0-dB antenna gain, at sunspot number 10 for January (12:00 LT).

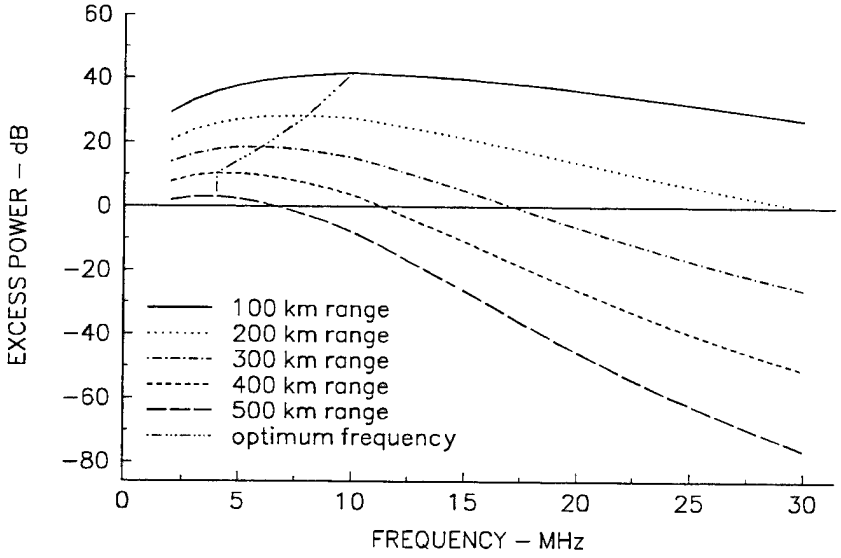

Figure 16. Excess power at a medium-noise area for a required SNR ratio of 45 dB, a required reliability of 90%, and a 0-dB antenna gain, at sunspot number 10, for January (24:00 LT).

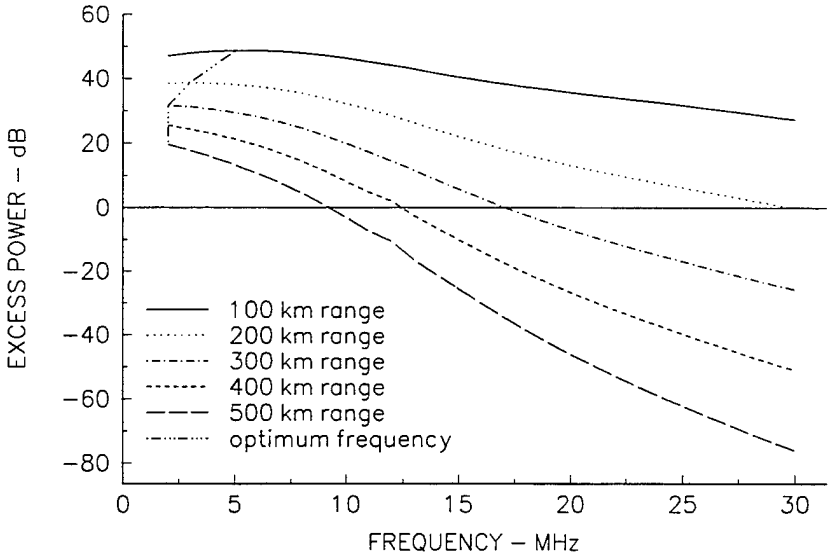

Figure 17. Excess power at a medium-noise area for a required SNR of 45 dB, a required reliability of 90%, and a 0-dB antenna gain, at sunspot number 160, for January (12:00 LT).

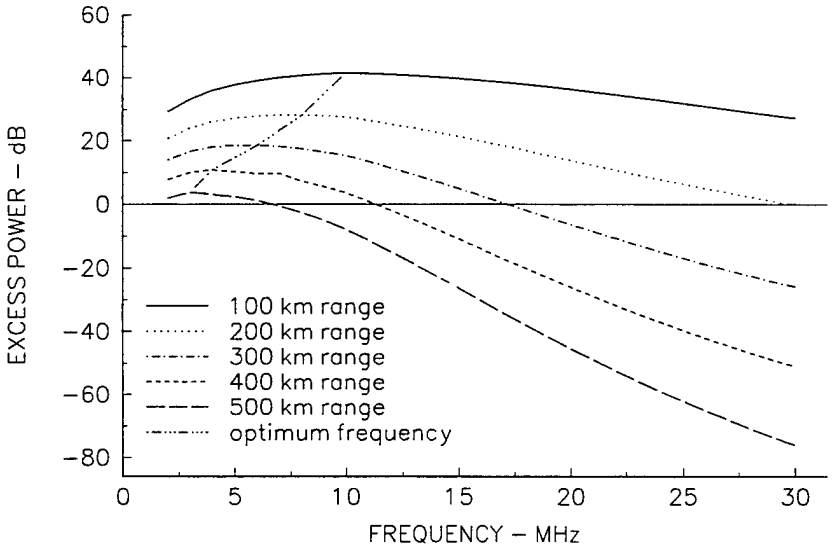

Figure 18. Excess power at a medium-noise area for a required SNR of 45 dB, a required reliability of 90%, and a 0-dB antenna gain, at sunspot number 160, for January (24:00 LT).

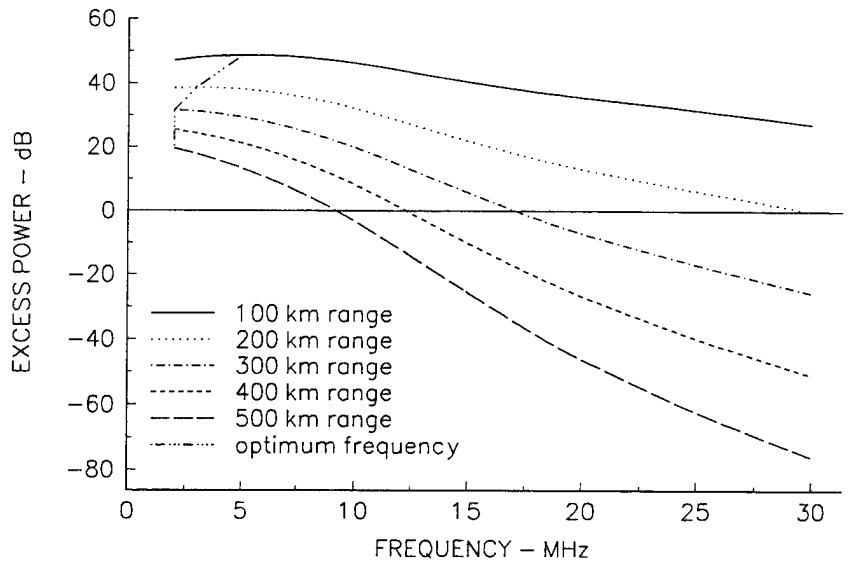

Figure 19. Excess power at a medium-noise area for a required SNR of 45 dB, a required reliability of 90%, and a 0-dB antenna gain, at sunspot number 10, for July (12:00 LT).

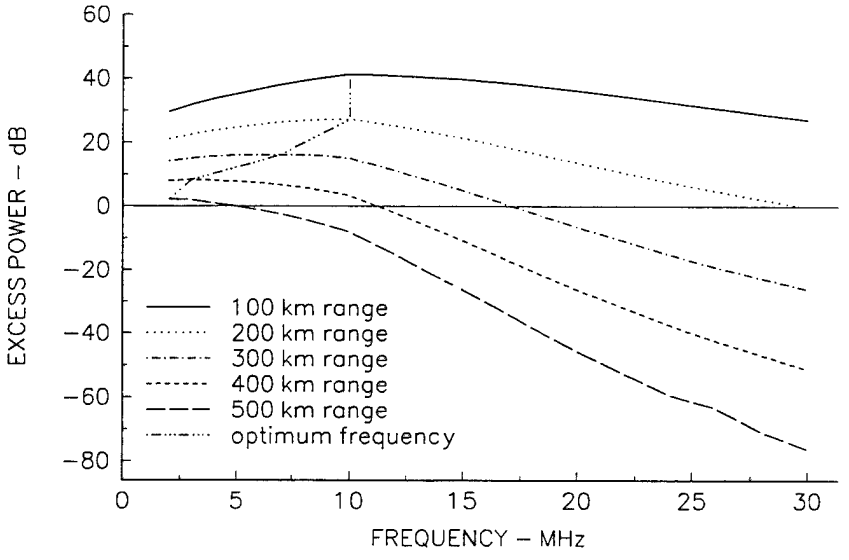

Figure 20. Excess power at a medium-noise area for a required S/N of 45 dB, a required reliability of 90%, and a 0-dB antenna gain, at sunspot number 10, for July (24:00 LT).

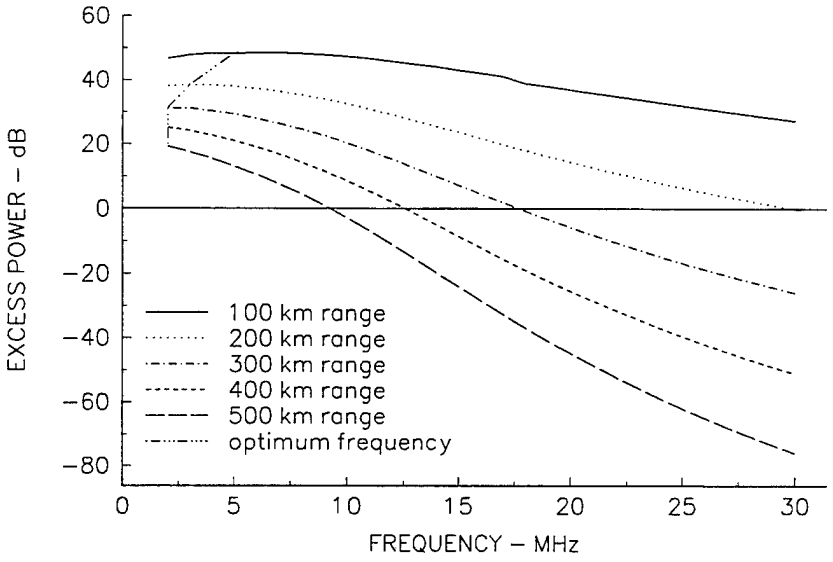

Figure 21. Excess power at a medium-noise area for a required SNR of 45 dB, a required reliability of 90%, and a 0-dB antenna gain, at sunspot number 160, for July (12:00 LT).

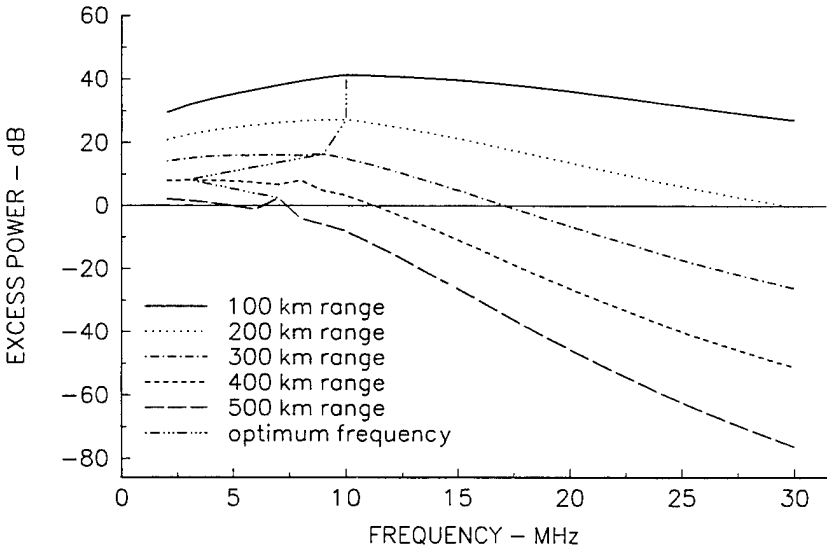

Figure 22. Excess power at a medium-noise area for a required SNR of 45 dB, a required reliability of 90%, and a 0-dB antenna gain, at sunspot number 160, for July (24:00 LT).

LOW RADIO NOISE LOCATION

Figures 23 through 30 show the range and frequency dependence of the excess available power for the low radio noise receiver location. Figures 23 through 26 are for January, whereas, figures 27 through 30 are for July. Figures 23, 25, 26, and 29 are for local noon. Figures 24, 26 28, and 30 are for local midnight. The shorter ranges of 100 and 200 km have positive excess available power at all frequencies for which calculations were made. Only in the figure for July at sunspot number 160 and at local noon is there any influence of an ionospheric mode. This occurs at 5 MHz. There is only a slight diurnal difference in the excess available power with the values higher at local midnight than local noon. This diurnal difference increases further and is more significant during July than during January. There is no apparent influence of the sky-wave mode of propagation at this low radio noise location.

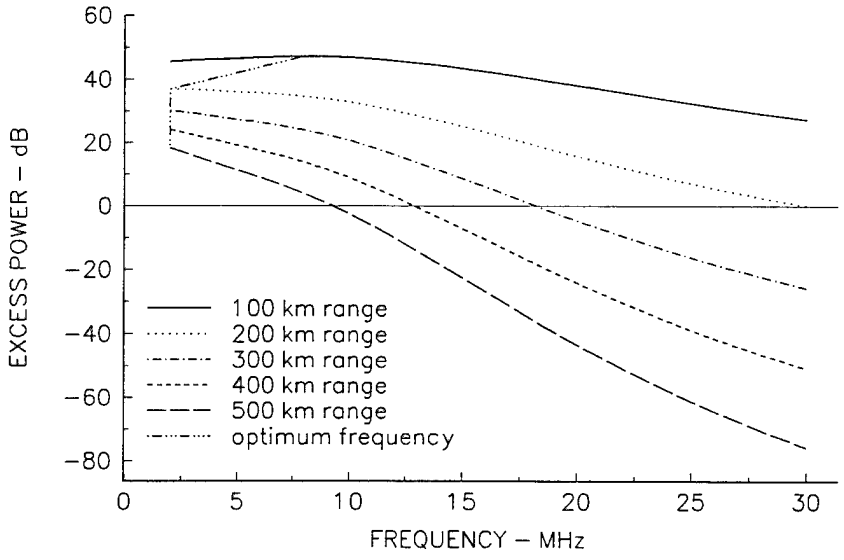

Figure 23. Excess power at a low-noise area for a required SNR of 45 dB, a required reliability of 90%, and a 0-dB antenna gain, at sunspot number 10, for January (12:00 LT).

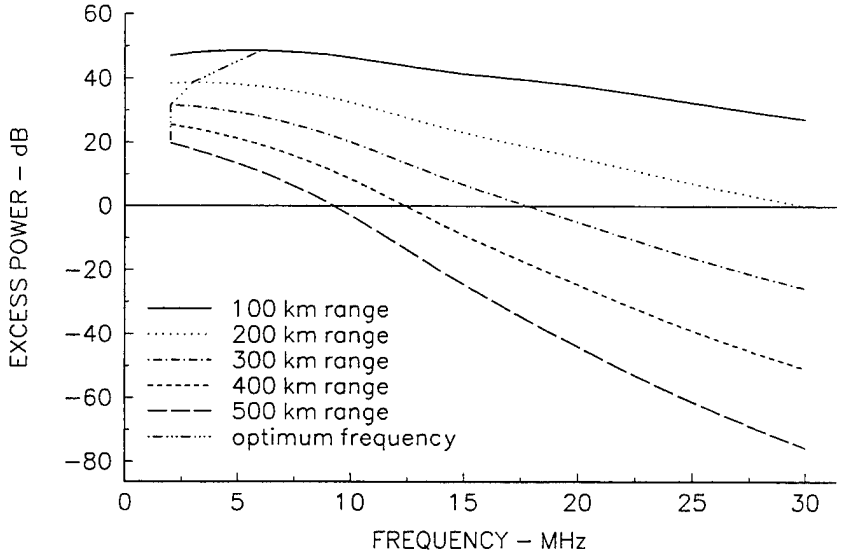

Figure 24. Excess power at a low-noise area for a required SNR of 45 dB, a required reliability of 90%, and a 0-dB antenna gain, at sunspot number 10, for January (24:00 LT).

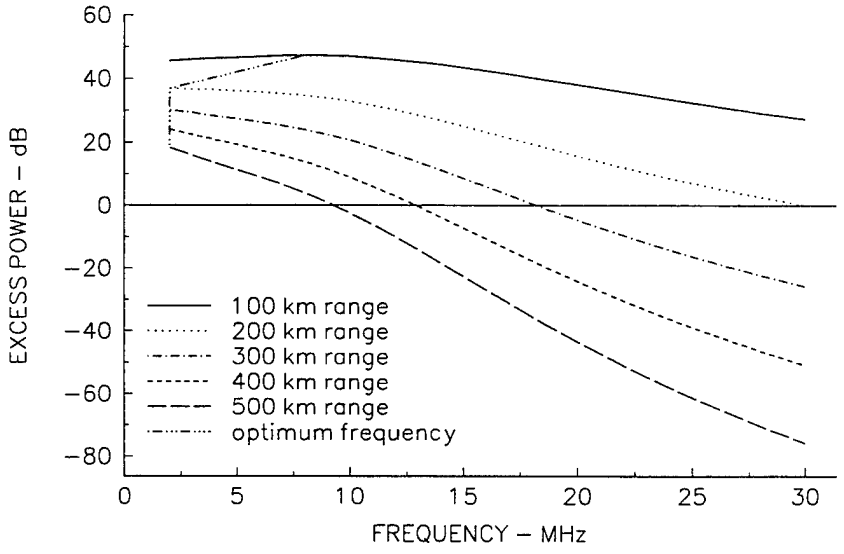

Figure 25. Excess power at a low-noise area for a required SNR of 45 dB, a required reliability of 90%, and a 0-dB antenna gain, at sunspot number 160, for January (12:00 LT).

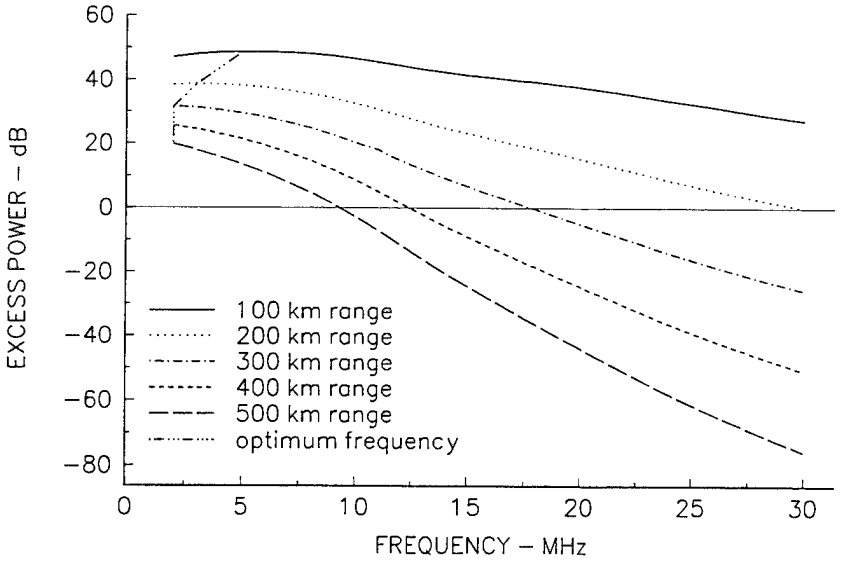

Figure 26. Excess power at a low-noise area for a required S/NR of 45 dB, a required reliability of 90%, and a 0-dB antenna gain, at sunspot number 160, for January (24:00 LT).

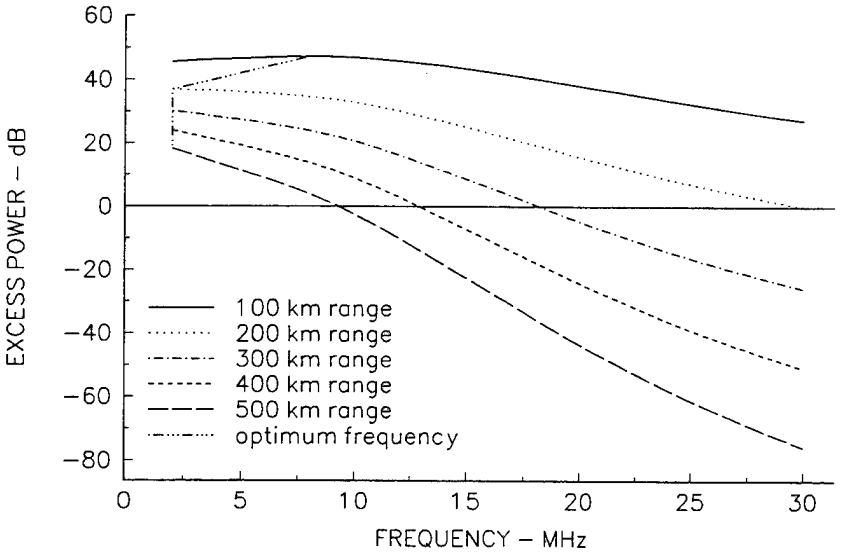

Figure 27. Excess power at a low-noise area for a required SNR of 45 dB, a required reliability of 90%, and a 0-dB antenna gain, at sunspot number 10, for July (12:00 LT).

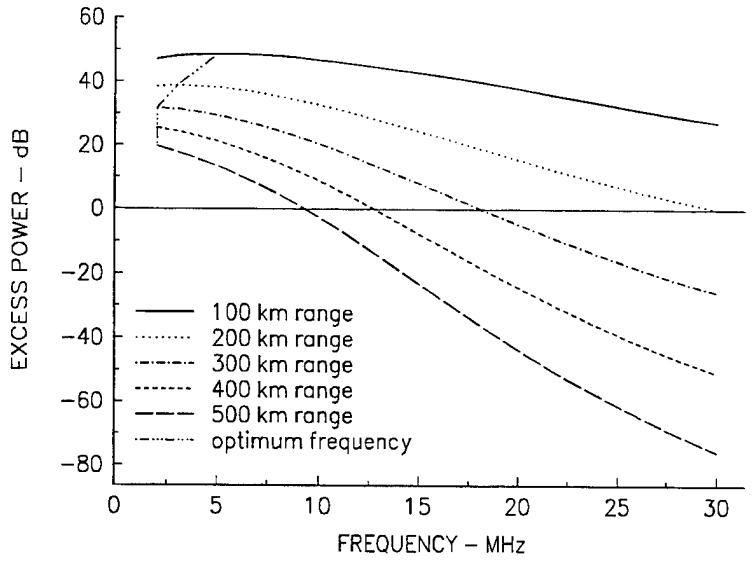

Figure 28. Excess power at a low-noise area for a required SNR of 45 dB, a required reliability of 90%, and a 0-dB antenna gain, at sunspot number 10, for July (24:00 LT).

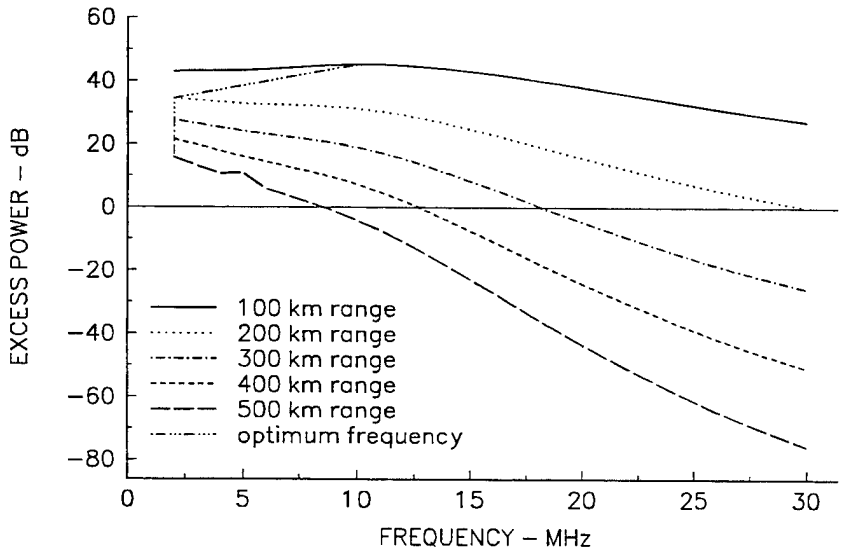

Figure 29. Excess power at a low-noise area for a required SNR of 45 dB, a required reliability of 90%, and a 0-dB antenna gain, at sunspot number 160, for July (12:00 LT).

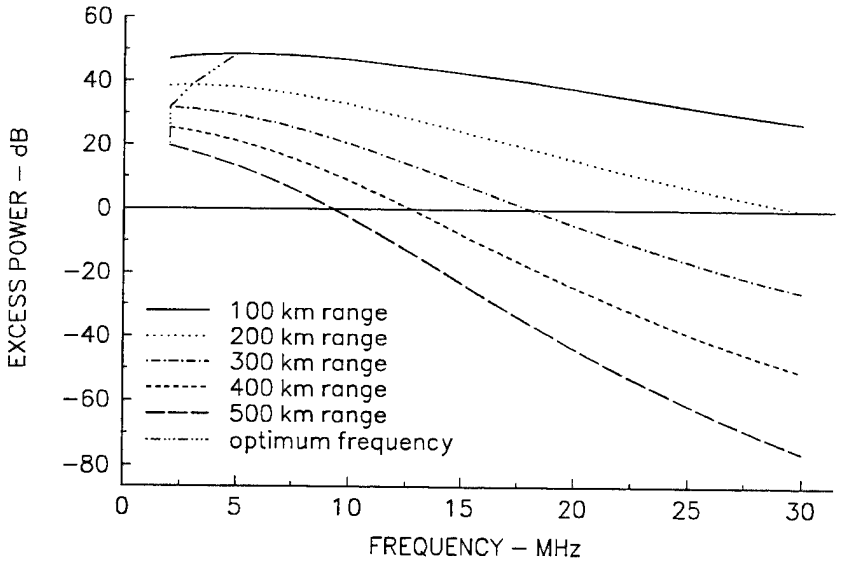

Figure 30. Excess power at a low-noise area for a required SNR of 45 dB, a required reliability of 90%, and a 0-dB antenna gain, at sunspot number 160, for July (24:00 LT).

HIGH-LATITUDE RECEIVER LOCATION

Figures 31 through 38 show the range and frequency dependence of the excess available power for the high-latitude receiver location. Figures 31 through 34 are for January, and figures 35 through 38 are for July. Figures 31, 33, 35, and 37 are for local noon. Figures 32, 36, 38, and 43 are for local midnight. There is little season, diurnal, or sunspot variation in these figures. This occurs because there is little seasonal or diurnal variation in the radio noise at these latitudes and because the ground wave has greater signal strength at these ranges at these latitudes. Although the excess available power was calculated for ionospheric storms conditions, the results were not plotted because the auroral absorption lessens the influence of the sky-wave modes even further.

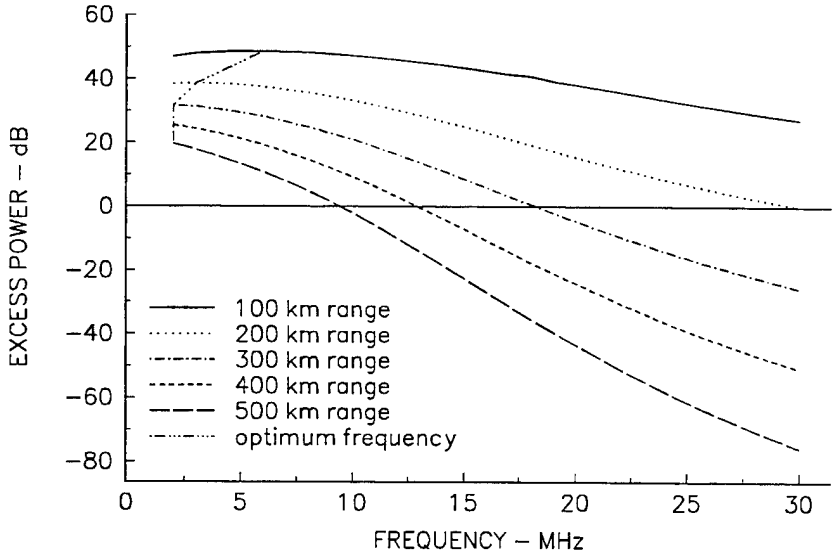

Figure 31. Excess power at a high-latitude noise area for a required SNR of 45 dB, a required reliability of 90%, and a 0-dB antenna gain, at sunspot number 10, for January (12:00 LT).

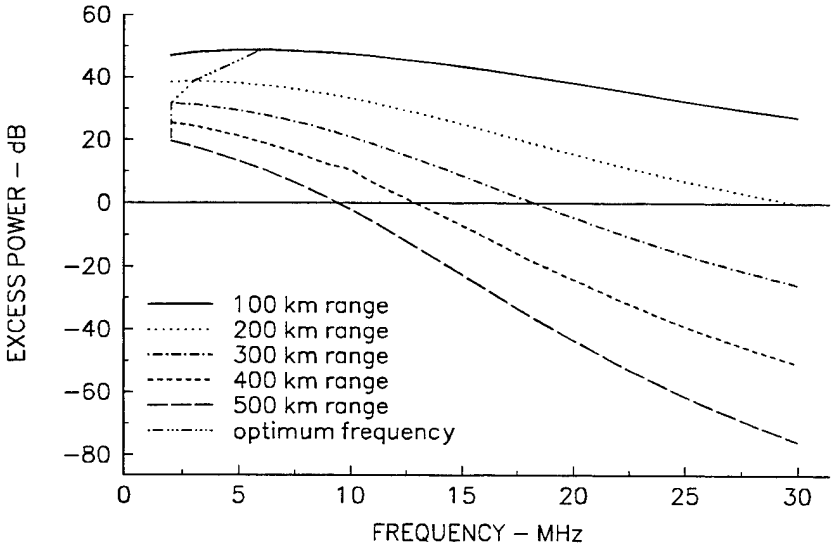

Figure 32. Excess power at a high-latitude noise area for a required SNR of 45 dB, a required reliability of 90%, and a 0-dB antenna gain, at sunspot number 10, for January (24:00 LT).

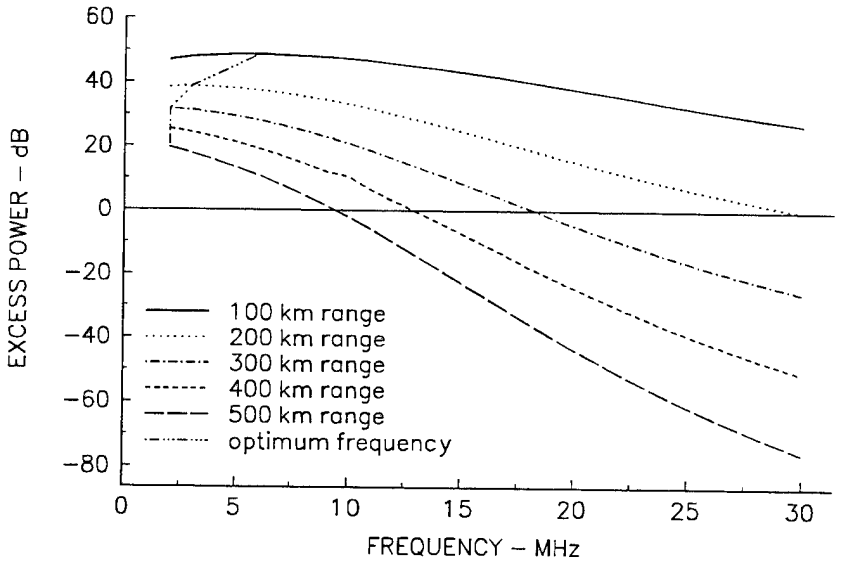

Figure 33. Excess power at a high-latitude noise area a required SNR of 45 dB, a required reliability of 90%, and a 0-dB antenna gain, at sunspot number 160, for January (12:00 LT).

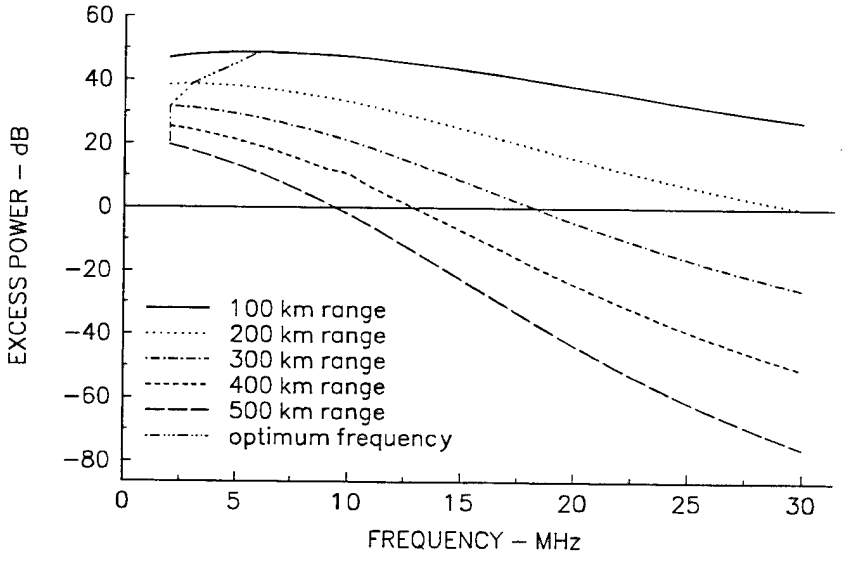

Figure 34. Excess power at a high-latitude noise area, for a required SNR of 45 dB, a required reliability of 90%, and a 0-dB antenna gain, at sunspot number 160, for January (24:00 LT).

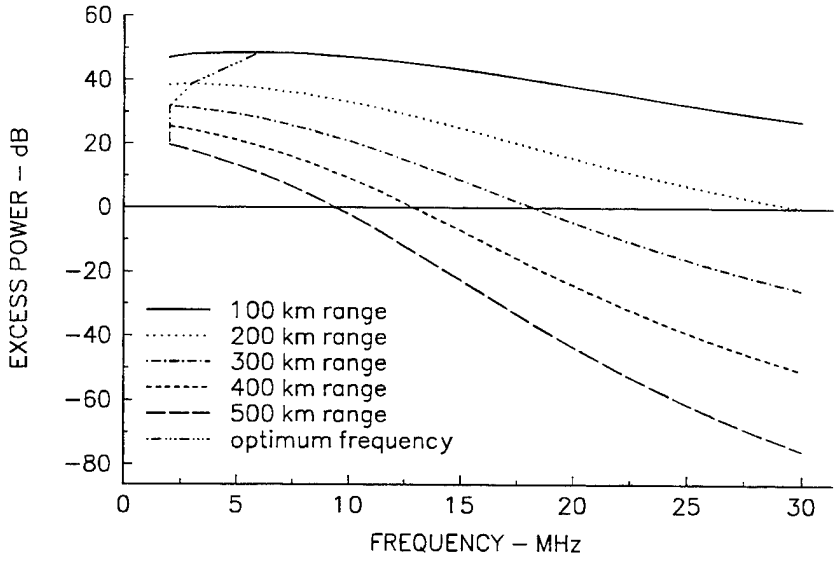

Figure 35. Excess power at an high-latitude noise area for a required SNR of 45 dB, a required reliability of 90%, and a 0-dB antenna gain, at sunspot number 10, for July (12:00 LT).

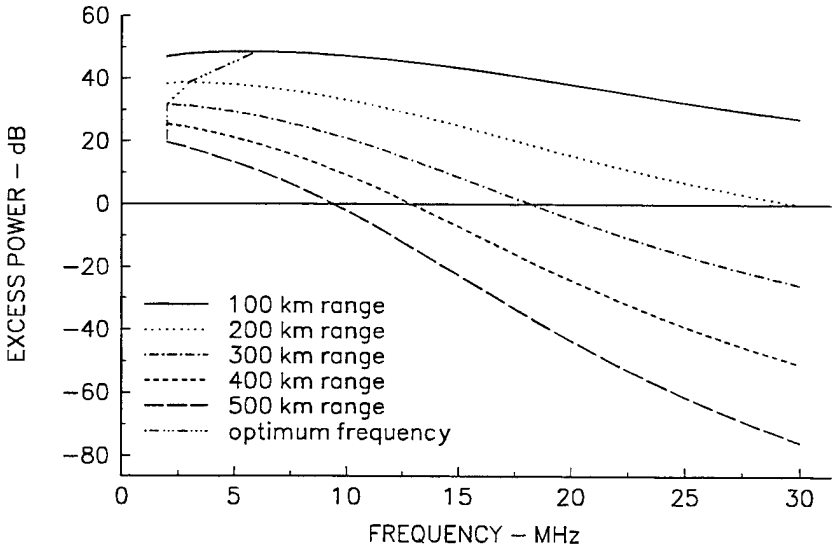

Figure 36. Excess power at an high-latitude noise area for a required SNR of 45 dB, a required reliability of 90%, and a 0-dB antenna gain, at sunspot number 10, for July (24:00 LT).

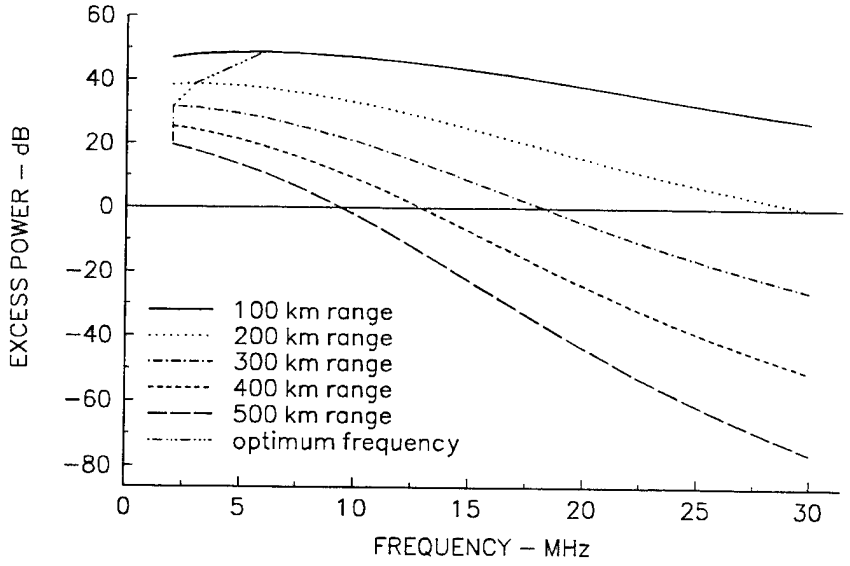

Figure 37. Excess power at an high-latitude noise area for a required SNR of 45 dB, a required reliability of 90%, and a 0-dB antenna gain, at sunspot number 160, for July (12:00 LT).

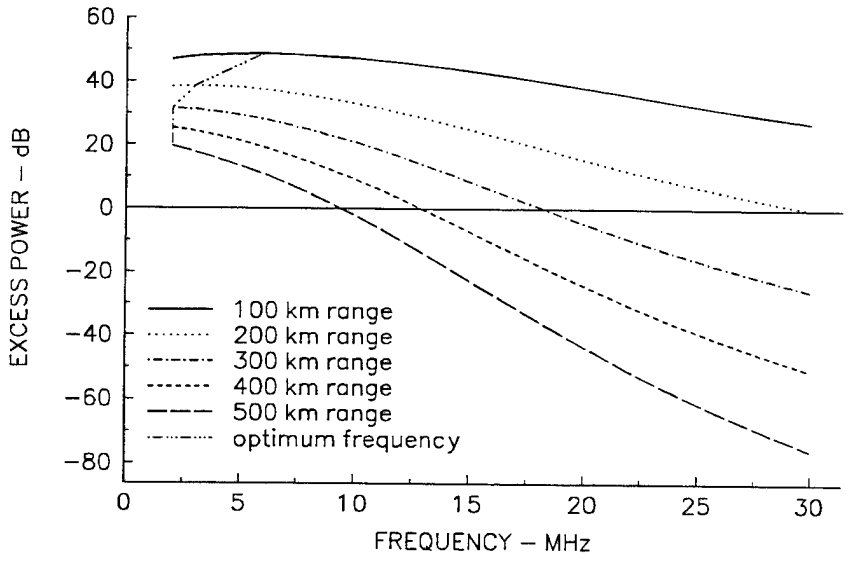

Figure 38. Excess power at a high-latitude noise area for a required SNR of 45 dB, a required reliability of 90%, and a 0-dB antenna gain, at sunspot number 160, for July (24:00 LT).

SKY-WAVE PROPAGATION ONLY

Figures 39 and 40 show the range and frequency dependence of the excess available power for sky-wave propagation only for the conditions of sunspot number 160 and July at the high radio noise receiver location. Figure 39 is for local noon, and figure 40 is a corresponding figure for local midnight. Figure 39 shows sky-wave propagation for range of 100 and 200 km. For the 100-km range, the SNR is very low, causing a deficit in the excess available power. For the 200-km range, sky-wave propagation is possible for more than one frequency. However, only the 10-MHz frequency is of sufficient SNR to satisfy the requirements of 45-dB SNR and a time availability of 90%. In figure 40, at local midnight there is sufficient excess power at the ranges of 100, 400, and 500 km for a very narrow range of frequencies. For the two longer ranges, only one frequency is usable. These two figures illustrate the type of sky-wave propagation known as the near-vertical incidence system (NVIS).

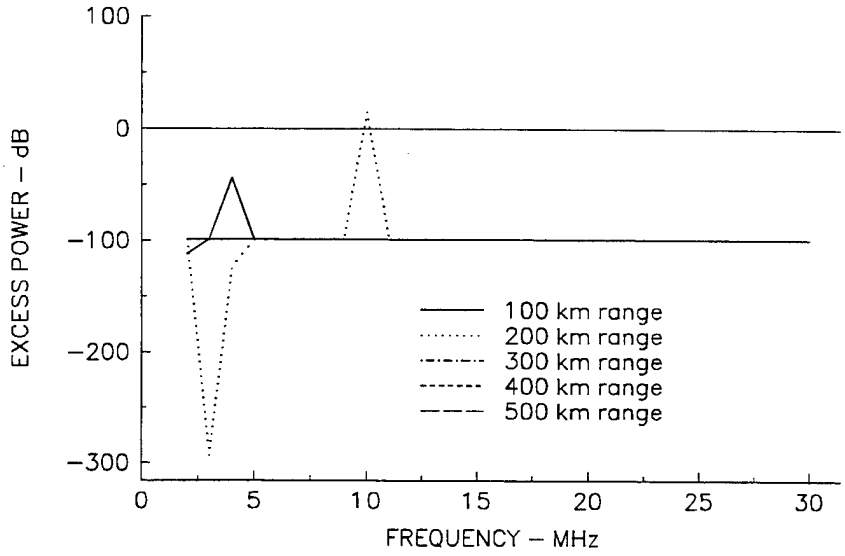

Figure 39. Excess power at a high-noise area—sky wave only, for a required SNR of 45 dB, a required reliability of 90%, and a 0-dB antenna gain, at sunspot number 160, for July (12:00 LT).

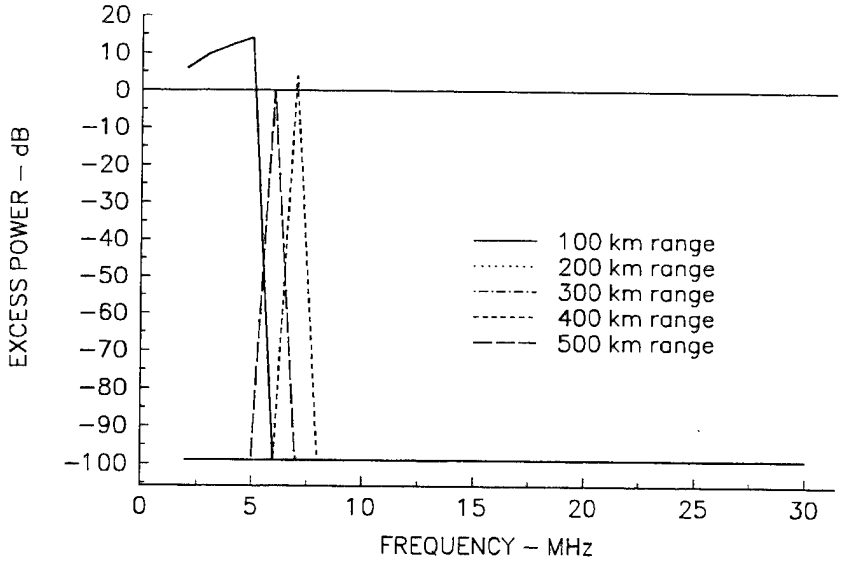

Figure 40. Excess power at an high noise area—sky wave only, for a required SNR of 45 dB, a required reliability of 90%, and a 0-dB antenna gain, at sunspot number 160, for July (24:00 LT).

AFFECTS OF SYSTEM TIME AVAILABILITY

One important parameter that affects the available excess system power is the required system time availability. The preceding figures were computed using a time availability of 90%. Figures 41 through 58 present the results of the analysis at the high radio noise location for the additional time availability values of 75%, 80%, 85%, and 95%. Figures 41 through 48 are similar to the figures presented above in that the excess power in dB versus frequency in MHz is presented as a function of range and optimum frequency for the new values of time availability. For each of the four values of time availability, two figures are given for sunspot number 160—one for local noon and one for local midnight at the receiver location.

Figures 41 and 42 are for a time availability of 75 % at local noontime and local midnight, respectively. If the corresponding results in figures 13 and 14 for a time availability of 90% are examined, one can see that there is a wider range of excess available power at 75% time availability than at 90% time availability. And at a time availability of 90% at local midnight, figure 14 shows that at 500 km, only a sky-wave mode is available, whereas, at a time availability of 75%, at local midnight a wider range of frequencies are available for a 500-km path. This trend continues as the time availability is increased to 95% in these figures. At a time availability of 95%, there are no usable frequencies at a range of 500 km at local midnight shown in figure 48.

These results indicated a need to separately display the results of the time availability analysis as a function of time availability at each of the five path ranges. Figures 49 through 58 show these results beginning with a path range of 100 km and continuing to 500 km. Each figure is for the high radio noise area at a sunspot number of 160. For each range, the results are presented first for local noon and then for local midnight. As one would expect, there is a

greater excess of available power for each range at a time availability of 75% than at 95%. There is a distinct difference frequency of maximum excess power for the two different times of day; local noon peaks at lower frequencies. As the range is increased, the difference in excess power between 75% and 95% time availability decreases considerably. Figure 58 shows dramatically the narrow range of usable frequencies available for a high radio noise location at local midnight.

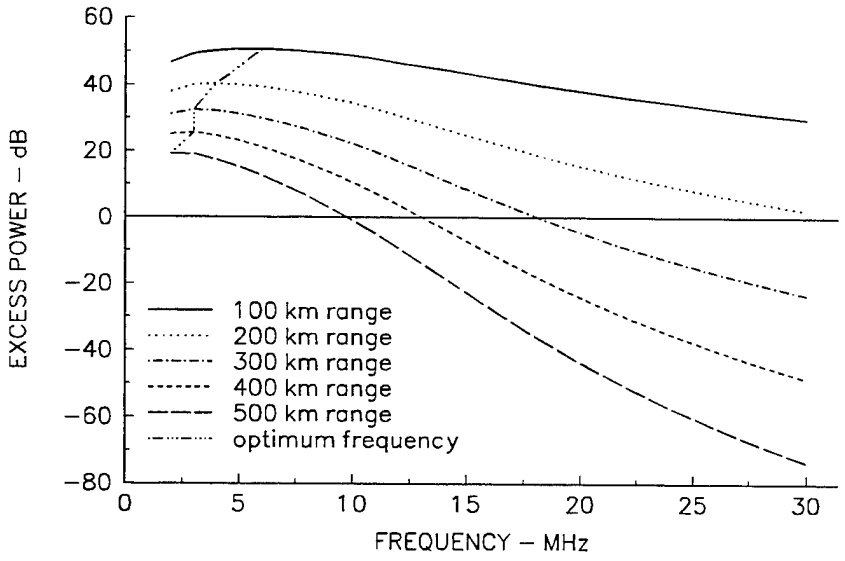

Figure 41. Excess power at a high-noise area for a required SNR of 45 dB, a required reliability of 75%, and a 0-dB antenna gain, at sunspot number 160, for July (12:00 LT).

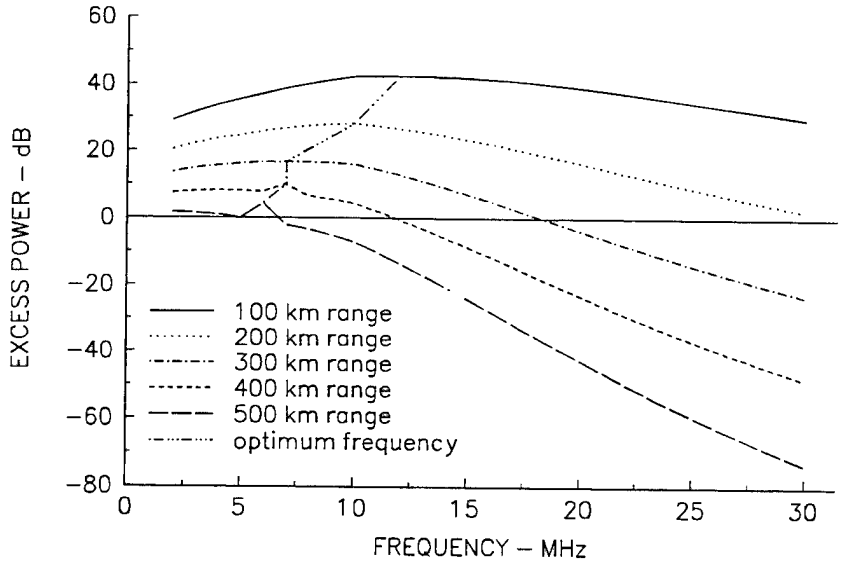

Figure 42. Excess power at a high-noise area for a required SNR of 45 dB, a required reliability of 75%, and a 0-dB antenna gain, at sunspot number 160, for July (24:00 LT).

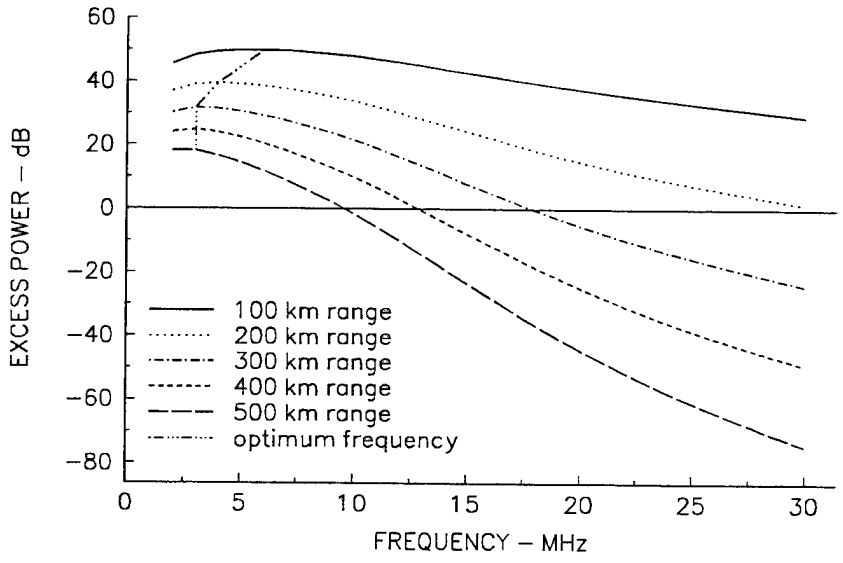

Figure 43. Excess power at a high-noise area for a required SNR of 45 dB, a required reliability of 80%, and a 0-dB antenna gain, at sunspot number 160, for July (12:00 LT).

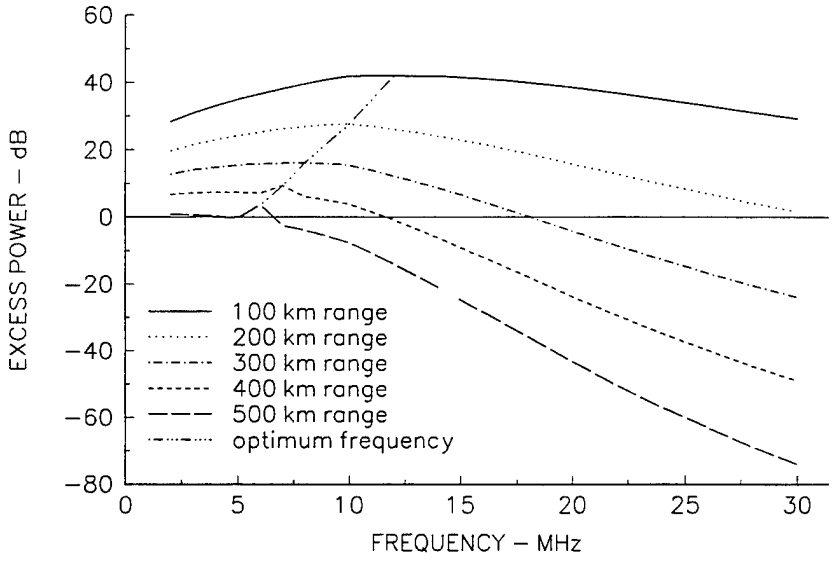

Figure 44. Excess power at a high-noise area for a required SNR of 45 dB, a required reliability of 80%, and a 0-dB antenna gain, at sunspot number 160, for July (24:00 LT).

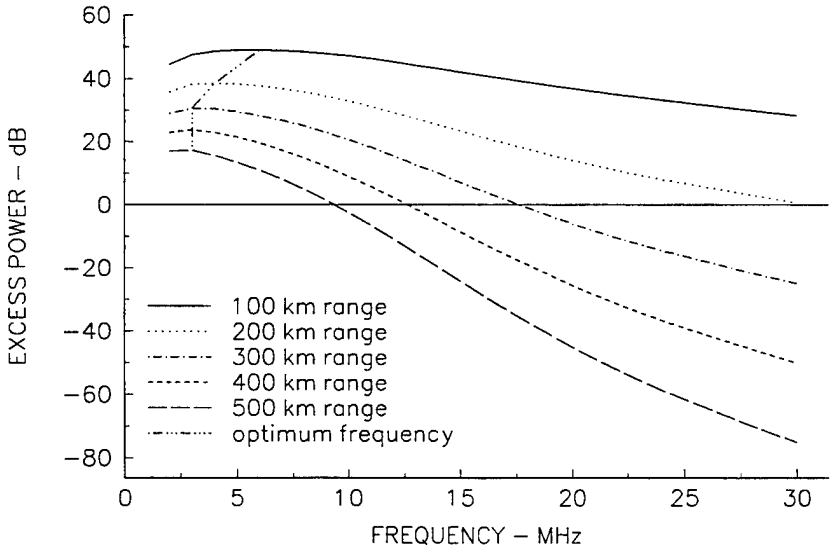

Figure 45. Excess power at a high-noise area for a required SNR of 45 dB, a required reliability of 85%, and 0-dB antenna gain, at sunspot number 160, for July (12:00 LT).

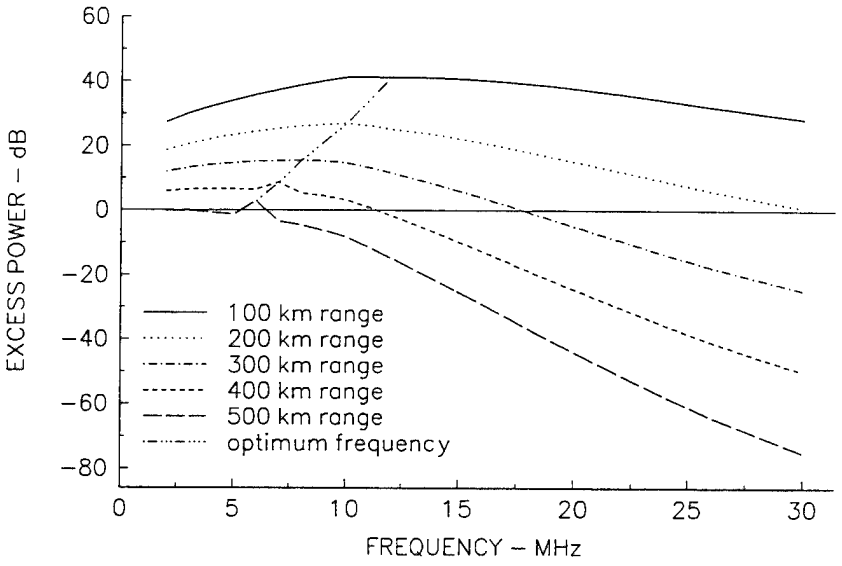

Figure 46. Excess power at a high-noise area for a required S/N of 45 dB, a required reliability of 85%, and a 0-dB antenna gain, at sunspot number 160, for July (24:00 LT).

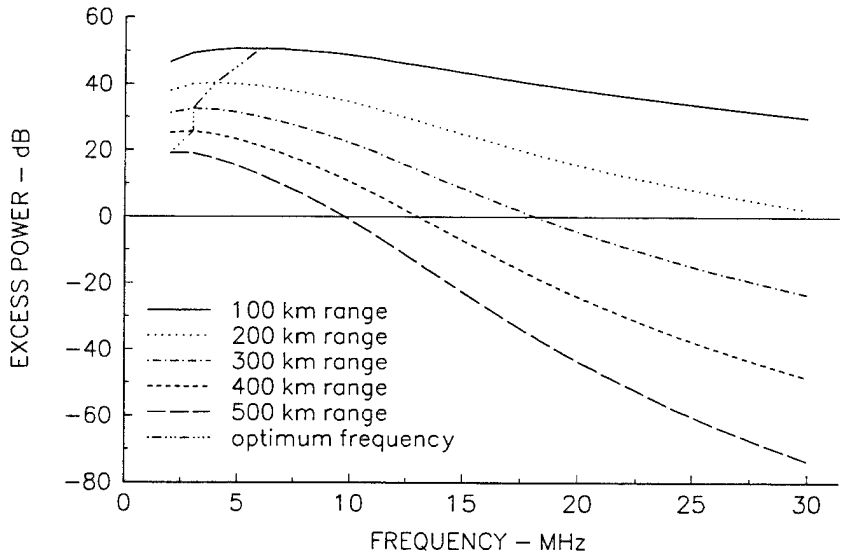

Figure 47. Excess power at a high-noise area,for a required SNR ratio of 45 dB, a required reliability of 95%, and a 0-dB antenna gain, at sunspot number 160, for July (12:00 LT).

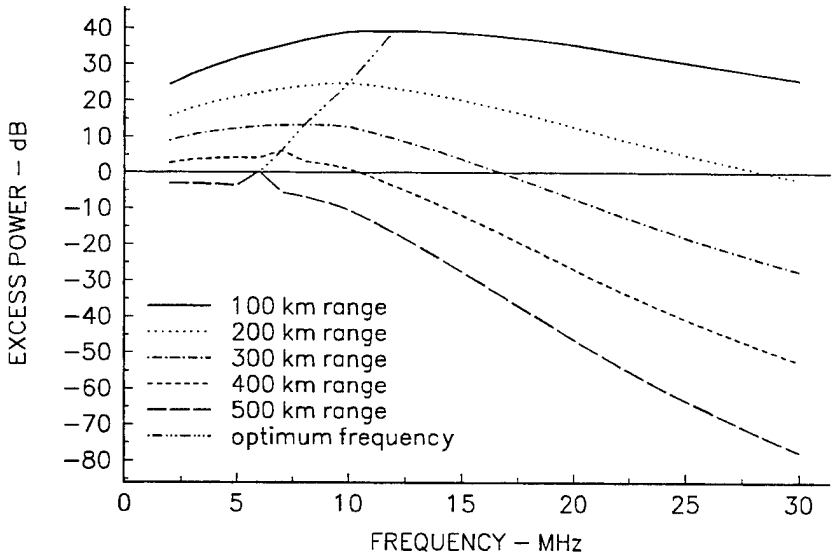

Figure 48. Excess power at a high-noise area for a required SNR of 45 dB, a required reliability of 95%, and a 0-dB antenna gain, at sunspot number 160, for July (24:00 LT).

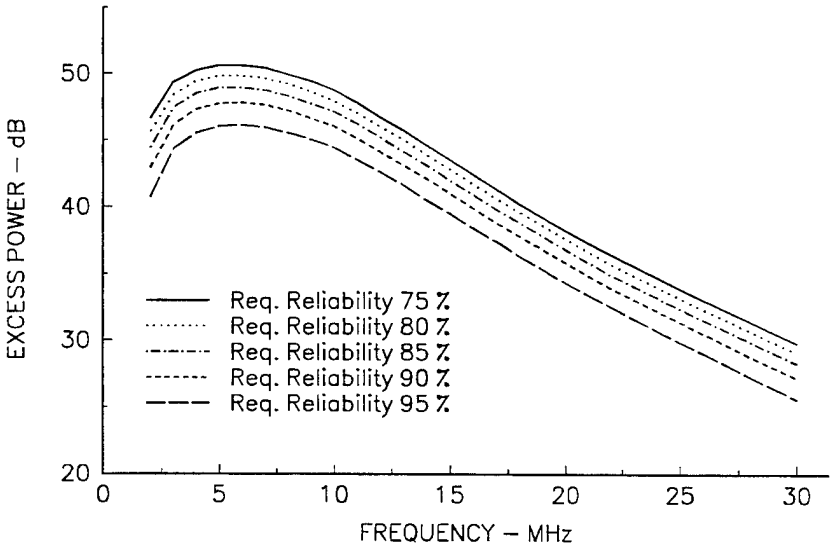

Figure 49. Excess power at a high-noise area for a required SNR of 45 dB, a path length of 100 km, and a 0-dB antenna gain, at sunspot number of 160, for July (12:00 LT).

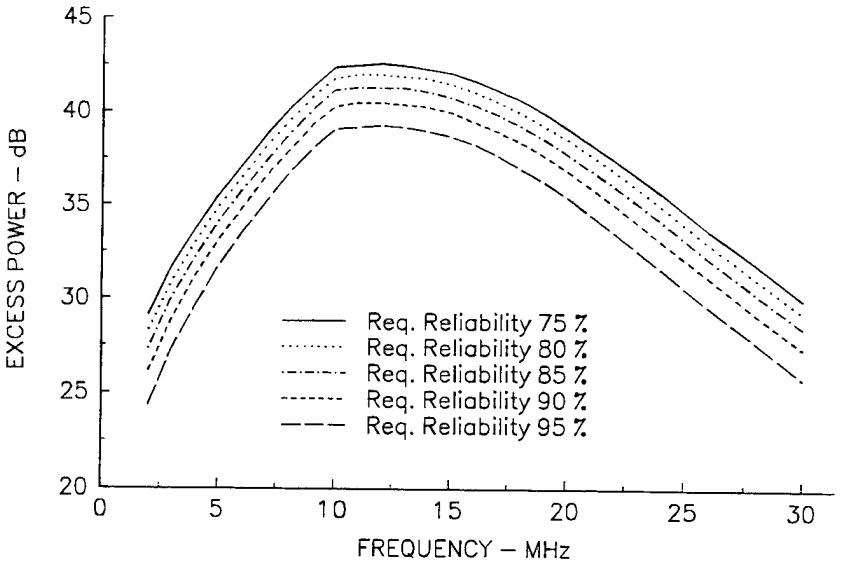

Figure 50. Excess power at a high-noise area for a required SNR of 45 dB, a path length of 100 km, and a 0-dB antenna gain, at sunspot number 160, for July (24:00 LT).

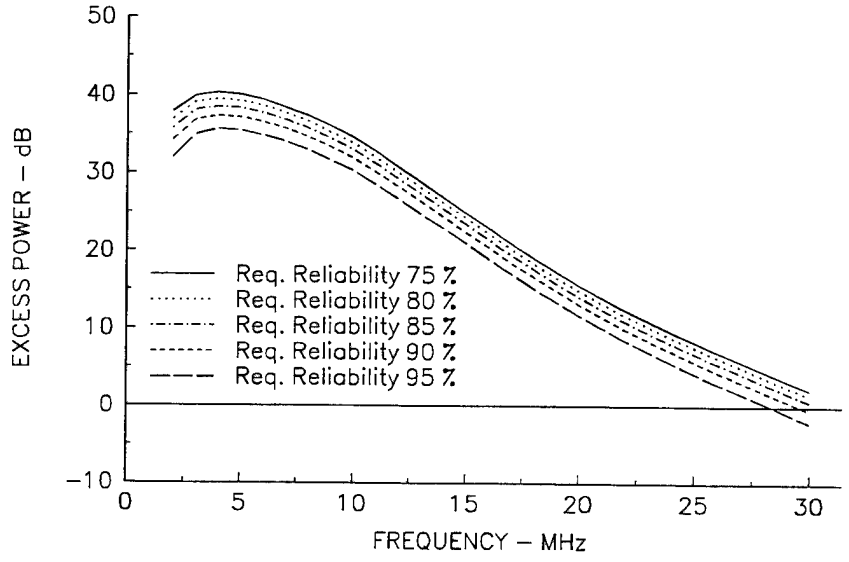

Figure 51. Excess power at a high-noise area for a required SNR of 45 dB, a path length of 200 km, and 0-dB antenna gain, at sunspot number 160, for July (12:00 LT).

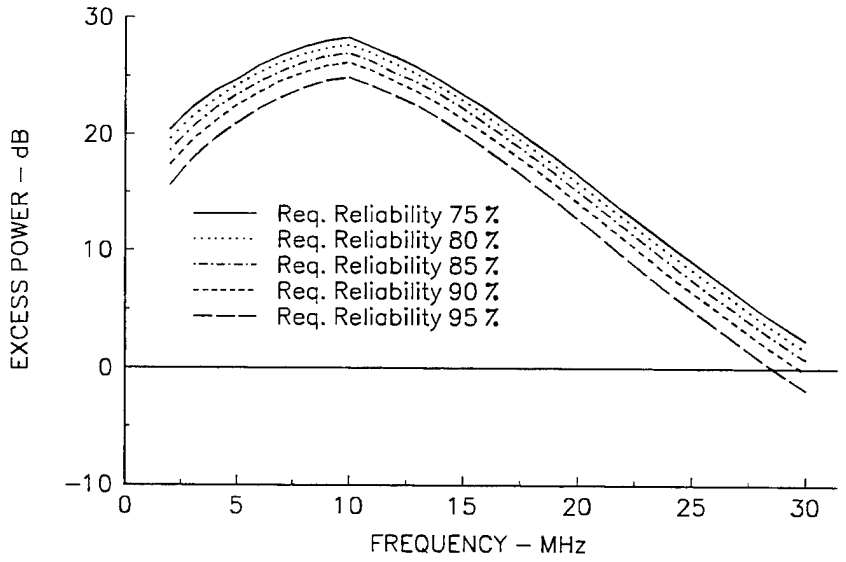

Figure 52. Excess power at a high-noise area for a required SNR of 45 dB, a path length of 200 km, and a 0-dB antenna gain, at sunspot number 160, for July (24:00 LT).

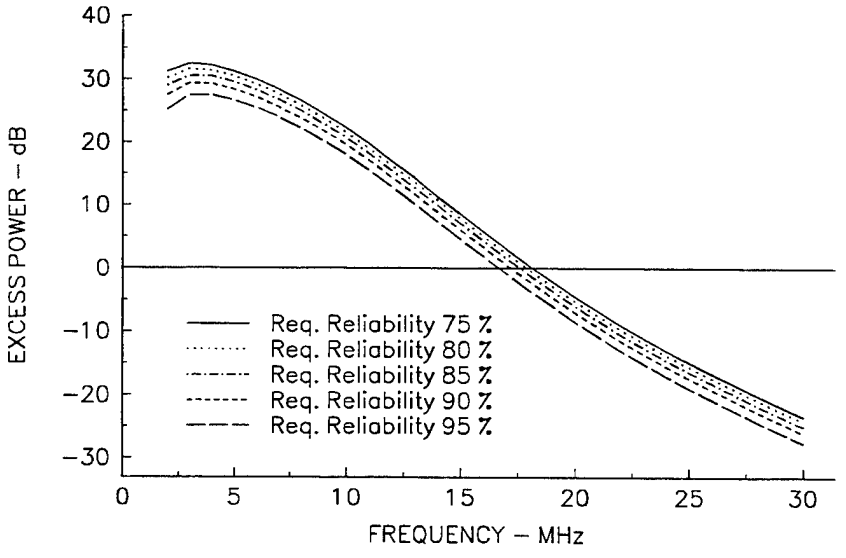

Figure 53. Excess power at a high-noise area for a required SNR of 45 dB, a path length of 300 km, and a 0-dB antenna gain, at sunspot number 160, for July (12:00 LT).

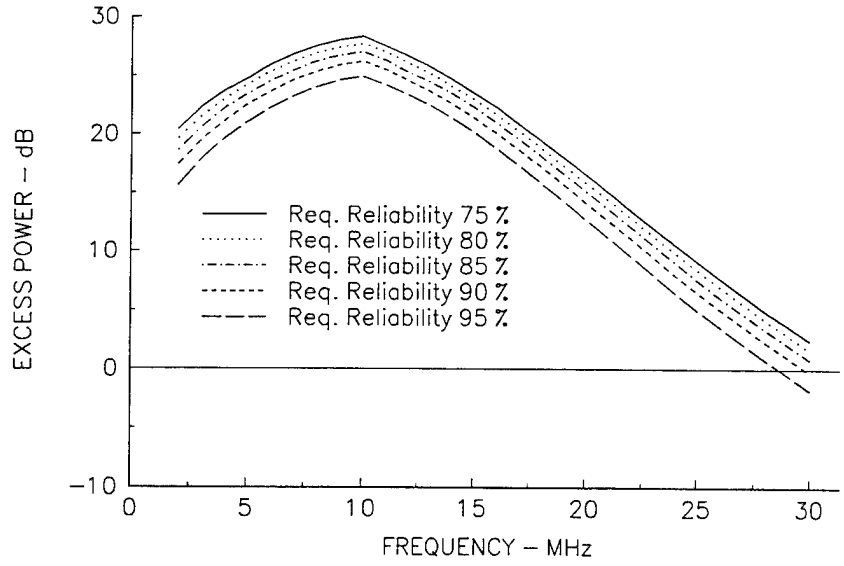

Figure 52. Excess power at a high-noise area for a required SNR of 45 dB, a path length of 200 km, and a 0-dB antenna gain, at sunspot number 160, for July (24:00 LT).

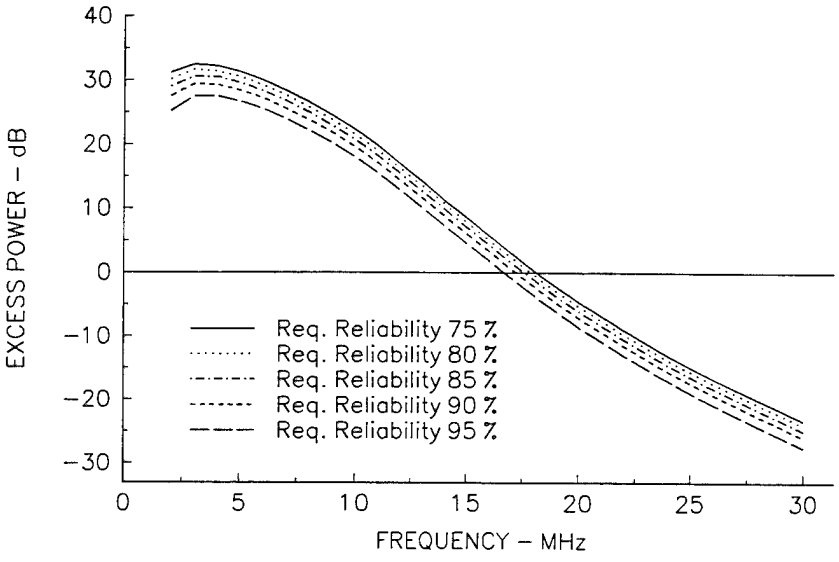

Figure 53. Excess power at a high-noise area for a required SNR of 45 dB, a path length of 300 km, and a 0-dB antenna gain, at sunspot number 160, for July (12:00 LT).

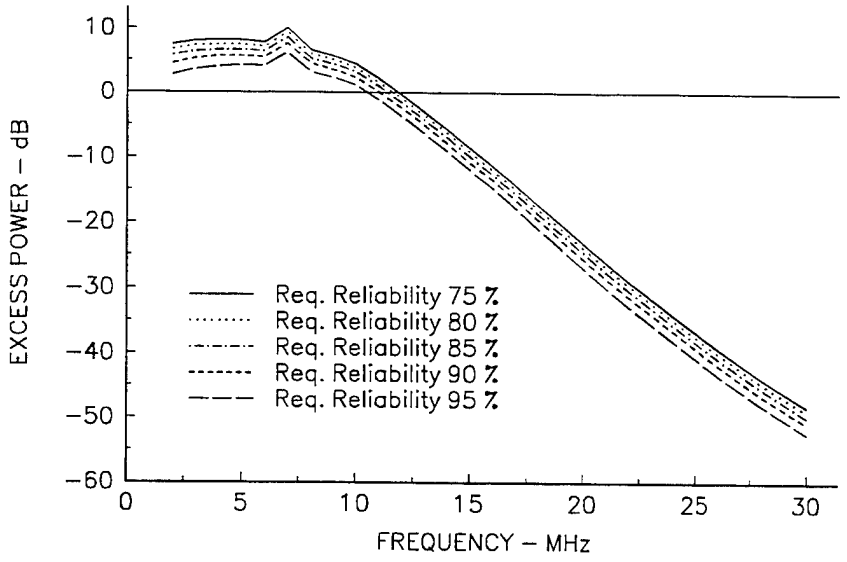

Figure 56. Excess power at a high-noise area for a required SNR of 45 dB, a path length of 400 km, and a 0-dB antenna gain, at sunspot number 160, for July (24:00 LT).

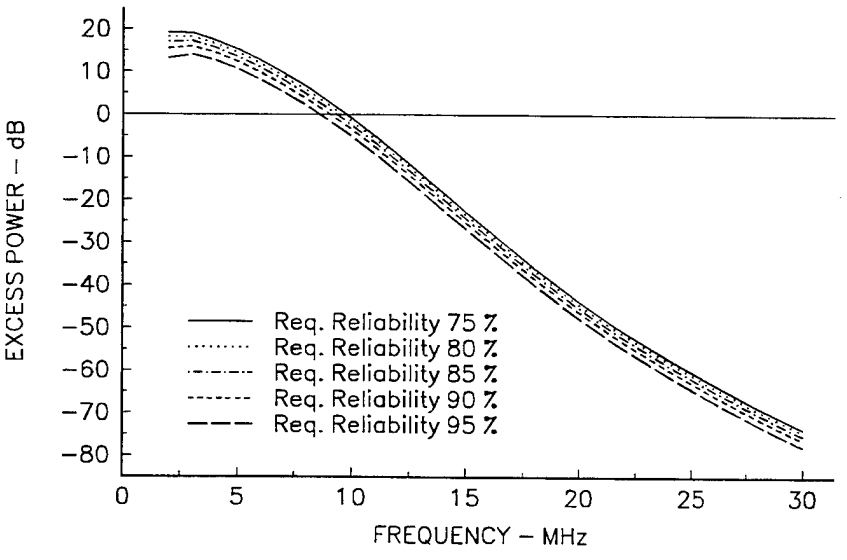

Figure 57. Excess power at a high-noise area for a required SNR of 45 dB, a path length of 500 km, and a 0-dB antenna gain, at sunspot number 160, for July (12:00 LT).

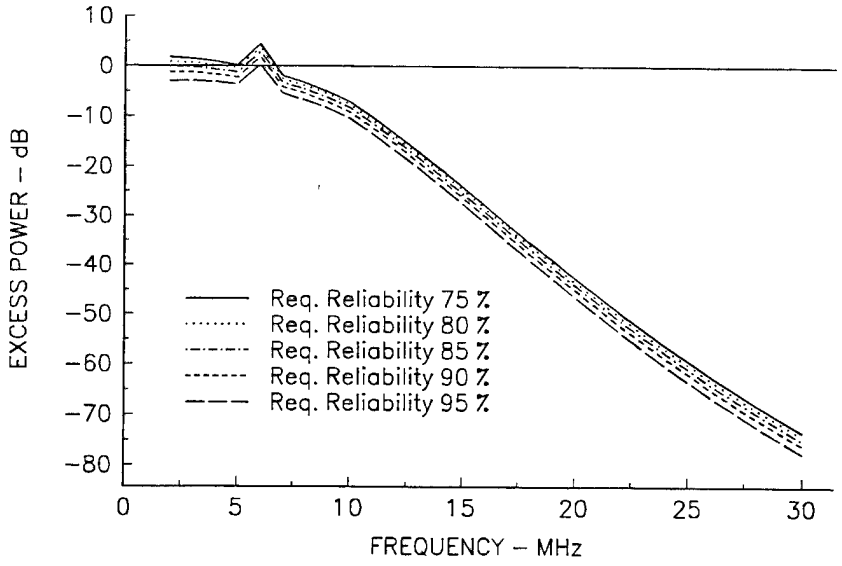

Figure 58. Excess power at a high-noise area for a required SNR of 45 dB, a path length of 500 km, and a 0-dB antenna gain, at sunspot number 160, for July (24:00 LT).

DISCUSSION

Three subjects in addition to the radio noise level at the receiver location discussed above affect the available excess transmission loss for surface wave transmission systems. First, the required signal-to-noise ratio (SNR) for various HF systems as it relates to the Results section above is important. The antenna gain as it relates to the Results section is also important. The affects of rough seas on the interpretation of the Results section is also important.

REQUIRED SIGNAL-TO-NOISE RATIO

The required SNR used in the analysis was 45 dB in a 1-Hz receiver noise bandwidth. Many communication systems have a required SNR far different from this value. Depending on whether the actual required SNR is higher or lower than this amount affects the interpretation of the results, particularly in the high radio noise area where the excess power is lowest.

The CCIR has compiled a table of required SNRs for various HF systems in Recommendation 339-6 (International Radio Consultative Committee, 1990). The required SNRs are given for both stable conditions and for fading conditions. The values for stable conditions applies in the case of ground-wave propagation when there is no strong sky-wave, as is the case in much of the analysis in the Results section. However, had the analysis been conducted here for the range 500 to 1,000 km, then it is very likely that there would be fading between the sky-wave and ground-wave modes in many instances. In this case the required SNR for fading conditions would be applicable. Beyond 1,000 km, where the sky-wave mode of propagation applies, the values for fading conditions are pertinent.

Tables 1 and 2 present a portion of the tables of Recommendation 339-6. Table 1 provides the required SNRs for the radio telephone service. Table 2 provides the required SNRs for the radio teletype service. To compare the results of the RESULTS section, subtract 45 dB from a value in either table. A positive value means the curves of figures 3 through 58 should be lowered by that amount. For instance, for J3E Telephony, a single-sideband suppressed carrier system with operator-to-operator grade of service and stable conditions, the required SNR is 47 dB. Subtracting 45 dB gives 2 dB. For this type of system, the curves in figures 3 through 58 should be lowered by 2 dB. Even for the high-noise area, this may make little difference. However, if we insist on good commercial quality, then the required SNR becomes 64 dB. The difference between this value and 45 dB is 19 dB. This difference is a significant amount. Only the shorter distances would be usable for a system of this type in the high radio noise area.

Other tables of required SNR in a 1-MHz receiver noise bandwidth are given by Teters et al. (1983). Many of the same HF systems are the same as those in tables 1 and 2. However, emission designators given there are the old CCIR designators rather than the current designators used in tables 1 and 2.

For reference purposes, advanced narrowband secure voice terminal (ANDVT) has a required SNR value of 41.8 dB in a 1-Hz receiver noise bandwidth (i.e., 7 dB in a 3-kHz receiver noise bandwidth), and DPSK Link 11 has a required SNR of 62.8 dB in a 1-Hz receiver noise bandwidth in the presence of atmospheric noise and Rayleigh-fading (i.e., 25 dB in a 6-kHz receiver noise bandwidth) (Olson, 1983).

ANTENNA GAIN

The antenna used in the analysis was an isotropic antenna on the sea surface. The analysis also assumed that the transmitting antenna had vertical polarization. The figures presented in the RESULTS section are not valid for horizontally polarized surface waves.

The calculation of the antenna gain for ground-wave propagation is complicated and depends on the frequency, the type of antenna, the height of the antenna above the ground, the characteristics of the ground above where the antenna is located, and the transmitted power. Milson (1976) discusses the effect of a conducting plane on the antenna gain, effective aperture, and radiation resistance with a summary of the consequences to ground-wave propagation for a Hertzian dipole, a half-wave dipole, and a small monopole. Based on Milson's work, Slator (1978) has applied the gain figures valid both to the transmit and receive antennas for the elementary dipole and its reflection. Milson gives the system transmission loss as the basic transmission loss minus the gain in free space of both the transmitting and receive antennas plus a factor, A'. The factor, A', is a function of the frequency, the height gain of the transmit and receive antennas, and orientation of the antenna element with respect to the vertical direction or normal to the surface. For a vertical electric dipole, the height gain is nearly 0 dB for heights above one-half wavelength above the ground, and A' thus becomes -6.02 dB for propagation in the equatorial plane (ground wave). At antenna heights below 0.1 wavelength, the height gain is approximately 3 dB; at an antenna height of one-quarter wavelength, the height gain is approximately 1 dB. Thus, for antennas on the ground, A' would become 0 dB. For both antennas at one-quarter wavelength above ground, A' would become 4 dB. The antenna gains would raise the curves in fiugres 3 through 58; A' would lower the excess power curves in these figures. Milson gives the directive gain of an Hertzian dipole as 1.76 dB and that of a half-wave dipole as 2.15 dB. Thus, for two vertical half-wave dipoles one-half wavelength above the earth, the curves would be raised upwards 10.32 dB, whereas, two vertical half-wave dipoles at ground level would raise the excess power curves by only 4.3 dB.

For ship-to-ship communications the situation is more complicated because of the uncertainty of the ships' directions. Horn (1971) has provided data for the average and standard deviation of four shipboard antennas. These values are presented in table 3. Also, the required protection factor for the uncertainty in the shipboard antenna pattern using a log-normal distribution frequency distribution for a time availability of 90% is given, assuming two like antennas on the path. The antenna gains are relative to a quarter-wave monopole over perfect ground. Thus, to adjust the average gain in the table to the reference used in the calculations for figures 3 through 58, it is necessary to subtract 5.15 dB (e.g., the average gain of a quarter-wave monopole over perfect ground relative to an isotropic antenna). The resulting average gain is -9.65 dB. Thus, the curves of figures 3 through 58 are adjusted downwards 9.65 dB for the antenna gain, downwards an additional 7.5 dB for the uncertainty in the shipboard antenna pattern, and upwards by 6.02 dB for system transmission loss adjustment for surface-wave propagation for antenna heights above one-half wavelength above the ground.

Table 1. Required SNRs for radiotelephone service.

Radio Telephone Description	Grade Of Service*					
	Operator-to-Operator**			Good Commercial Quality		
	Stable Condition (dB)	No Diversity (dB)	Dual Diversity (dB)	Stable Condition (dB)	No Diversity (dB)	Dual Diversity (dB)
A3E Telephony - Double sideband	50	51	48	67	75	70
R3E Telephony - Single-sideband reduced carrier	48	49	46	65	73	68
J3E Telephony - Single-sideband suppressed carrier	47	48	45	64	72	67
B8E Telephony - Independent-sideband 2 channels	49	50	47	66	74	69
B8E Telephony - Independent-sideband 4 channels	50	51	48	67	75	70

*Required Signal-to-Noise Ratio in required bandwidth relative to noise in a 1-Hz receiver noise bandwidth (dB),
**For 90% intelligibility of related words.

Table 2. Required SNRs for radioteletype service.

Radio Teletype Description	Grade Of Service* Character Error Rate**					
	10^{-2}			10^{-4}		
	Stable Condition (dB)	No Diversity (dB)	Dual Diversity (dB)	Stable Condition (dB)	No Diversity (dB)	Dual Diversity (dB)
F1B Telegraphy - 50 bauds, printer, 2D= 200 Hz to 400 Hz	45	53	45	56	74	59
F1B Telegraphy - MFSK 33-tone, ITA2 10 characters/s	23	37	29	26	52	39
F1B Telegraphy - MFSK 12-tone, ITA5 10 characters/s	26	42	32	29	56	42
F1B Telegraphy - MFSK 6-tone, ITA2 10 characters/s	25	41	31	28	55	41
J7B Multichannel - V.F. Telegraphy, 16 channels, 75 bauds each	59	67	59	69	87	72
B7W Composite - 16 channels, 75 bauds each, 1 telephony channel	60	68	60	70	88	73

*Required signal-to-noise ratio in required bandwidth relative to noise in a 1-Hz receiver noise bandwidth (dB).
**No error control schemes, power assumed equally divided between channels.

Table 3. Shipboard antenna gain characteristics.

Antenna Type	Average Gain (dB)	Standard Deviation (dB)	Protection Factor (dB)
Fiberglass twin whip	-4.3	4.1	7.4
Modified twin fan	-4.1	3.5	6.3
Forward twin fan	-4.9	3.8	6.9
Trussed whip	-4.8	5.2	9.4
Average	-4.5	4.2	7.5

AFFECTS OF ROUGH SEAS

The analysis results presented in the Results section are for a perfectly smooth (planar or spherical) interface between the air and ground or water. It is important to consider the impact of the sea roughness on the curves in figures 3 through 58. Barrick (1970, 1971a, and 1971b) has developed a method of analyzing radiation and propagation above a surface employing an effective surface impedance to describe the effect of the sea roughness boundary. The resulting effective surface impedance consists of two terms: (1) the impedance of the lower medium when the surface is perfectly smooth; and (2) a second term accounting for roughness. The latter term can be complex in general and depends on the strengths of the roughness spectral components present.

At HF, the longer, higher gravity waves will obviously play an important role in the interaction process. Such ocean waves owe their existence to winds blowing above the surface. However, a precise, qualitative relationship between the roughness heights and the winds is complicated by several factors. First, it takes several hours for waves to build up to their full strength or become fully arisen under the influence of the wind. For example, the minimum duration time for a sea state 2 (10-knot wind) to become fully arisen is 2.4 hours; for a sea state 6 (30-knot wind) the minimum duration time for the sea to become fully arisen is 24 hours (Myers et al, 1969). The homogeneity of the wave spectrum aroused in a given region depends on the spatial area over which the winds are blowing; this area is called the 'fetch.' Myer et al (ibid) give a minimum fetch of 19 km for sea state 2 and of 537 km for sea state 6. Part of the roughness is due to winds or storms located far away in space and/or time from the region of interest; this effect is called 'swell' and is usually quite directional. For hurricane winds and also often whole gale and storm winds, required fetches and durations are rarely at-

tained. In such cases, sea states are not fully arisen. Table 4 provides additional useful data that relate sea state to wind and sea conditions for a fully arisen sea (Myers et al, 1969). The values of average wave height given in the source were converted to meters; the values given in the source in nmi were converted to km.

Because the models of ocean wave height spectrum developed by oceanographers over the years neglect the effect of limited fetch and swell, and since they assume the winds have been blowing sufficiently long that the sea is fully arisen, the results of Barrack's technique would apply more often to sea state 2 rather than sea state 6. Another consideration is the sea state fetch distance relative to the path distance. If the path distance is shorter than the fetch distance, then the effect of sea state can be applied to the whole path. However, if the path distance is longer than the fetch distance, then some methods, such as that of Millington (1949), should be applied to account for the differences along the path. In practice this is usually ignored, resulting in a pessimistic predication of the added transmission loss due to rough seas.

Barrick employed the expression for the effective surface impedance to calculate the ground-wave basic transmission loss due to sea state. To obtain a rough estimate of this loss, he employed for the height spectrum of the ocean, two wind-wave spatial spectrum models. For the first, the Neumann-Pierson model, the most changes in surface impedance occur for propagation in the upwind-downwind direction. The values of the effective surface impedance obtained from the Phillips semi-isotropic, wind-wave spectrum lie between the values of the Neumann-Pierson model for the upward-downwind and crosswind directions.

Barrick (1970 and 1971b) used values of surface impedance calculated for the Phillips spectrum to predict the excess transmission loss due to the sea state, the difference between the basic transmission loss above a rough sea, and the value above a smooth sea. He showed several figures each computed at different frequencies that gave this loss at difference sea states as a function of range between transmitter and receiver. First, a negative loss is observed at the lower HF frequencies of 3 to 5 MHz. A negative loss indicates an increase in signal strength; this effect occurs where the ocean waves present have lengths small in terms of the radio wavelength. Sea state loss appears to be the greatest at about 10 to 15 MHz and seems to decrease above this frequency. At 15 MHz, the increase in loss can be as much as 15 dB at 100 nmi.

Barricks' presentation of his results included only seven frequencies (3 MHz, 5 MHz, 7 MHz, 10 MHz, 15 MHz, 20 MHz, 30 MHz, and 50 MHz). The results were presented as the added transmission loss versus range. A separate figure was used for each frequency, making it difficult to visualize the frequency variation.

The approach taken here was to plot the added transmission loss versus frequency for each of the five ranges used in figures 3 through 58. The results can be used to adjust the excess transmission loses. The surface impedance model of appendix A was used in the ground- wave program GW used to produce figures 3 through 58 to create a separate figure for each of the six sea states. Figures 59 through 64 show the added transmission loss for wind speeds of 5, 10, 15, 20, 25, and 30 knots, respectively, for antennas located just above the surface, and for the Phillips' isotropic ocean-wave spectrum. In all these figures there is an amplification of the signal at the lower frequencies, and then at a cross-over frequency, the added transmission loss increases to a maximum and then decreases slightly.

The added transmission loss is lowest for the lowest sea states and highest for the highest sea state. The maximum added transmission loss is always for the longest range. In figure 59, winds blowing at 5 knots show the maximum added transmission loss as just over 3 dB for frequencies above 9 MHz with the maximum value occurring at about 17.5 MHz. Note also the amplification of the signal strength at frequencies below 9 MHz. In figure 60, winds blowing at 10 knots show the maximum added transmission loss as about 9.8 dB at about 16 MHz. Below 7.5 MHz the signal strength is moderately amplified. In figure 61, the winds blowing at 15 knots show the maximum added transmission loss for a 500-km range is 15.1 dB at 17 MHz. Below 6 MHz there is a slight amplification of the signal. In figure 62, the winds blowing at 20 knots show that the maximum added transmission loss of 18.9 dB occurs at 17 MHz; there is little added transmission loss at frequencies below 4 MHz. In figure 63, winds blowing at 25 knots show that the maximum added transmission loss for 500 km is about 22.0 dB at a frequency of 16 MHz. Again there is no appreciable added transmission losses at frequencies below 4 MHz. In figure 64, winds blowing at 30 knots show a maximum added transmission loss of about 25.4 dB at about 14 MHz with no appreciable added transmission loss at frequencies below 4 MHz.

As the optimum frequency shown in figures 3 through 58 does not occur at frequencies above 10 MHz even in the worst case, the effect of sea state roughness is not as serious as it would seem for communication systems that attempt to operate at these frequencies. This is particularly true in light of the comments given concerning the time for the sea to become fully arisen and the sea state fetch distance to path length difference. However, as some systems may not operate at these frequencies, the effect of sea state roughness must be considered.

Table 4. Wind and sea scales for a fully arisen sea.

Sea State	Description	Wind			Sea			
		Description	Range Knots	Average Wind Velocity (knots)	Average Wave Height (meters)	Average Period (Sec)	Minimum fetch (km)	Minimum duration (hr)
0	Sea like a mirror.	Calm	Less than 1	0	0			
1	Small wavelets, still short but more pronounced; crests have a glassy appearance, but do not break.	Light breeze	4-6	5	0.05	1.4	15	39 min
2	Large wavelets, crests begin to break. Foam of glassy appearance, but do not break.	Gentle breeze	7-10	10	0.27	2.9	19	2.4
3	Small waves, becoming larger; fairly frequent white horses.	Moderate breeze	11-16	14	0.61	4.0	52	5.2
4	Moderate waves, taking a more pronounced long form; many white horses are formed (chance of some spray)	Fresh breeze	17-21	19	1.31	5.4	120	9.2
5	Large waves begin to form; the white foam crests are more extensive everywhere (probably some spray)	Strong breeze	22-27	24.5	2.50	7.0	304	15
6	Sea heaps up and white foam from breaking waves begin to be blown in streaks along the direction of the wind (spindrift begins to be seen)	Moderate gale	28-33	30.5	4.27	8.7	537	24

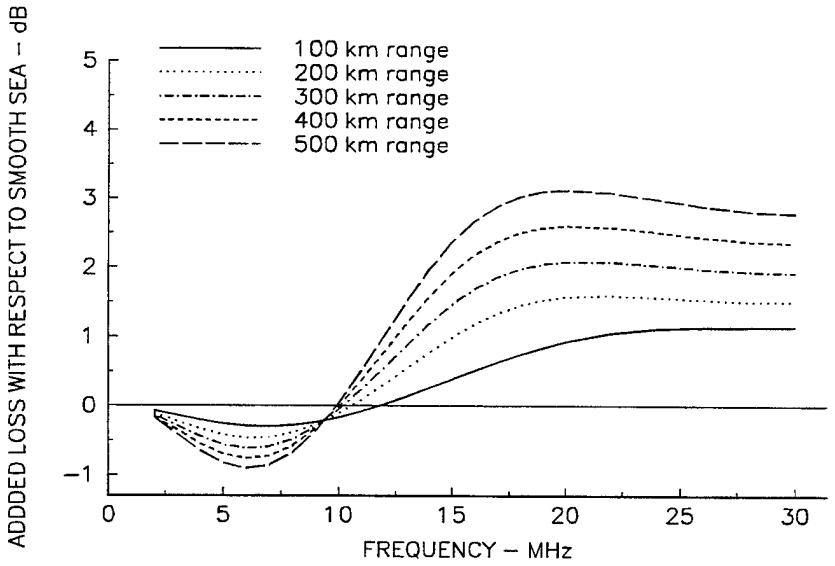

Figure 59. Added transmission loss due to sea state with 5-knot winds blowing.

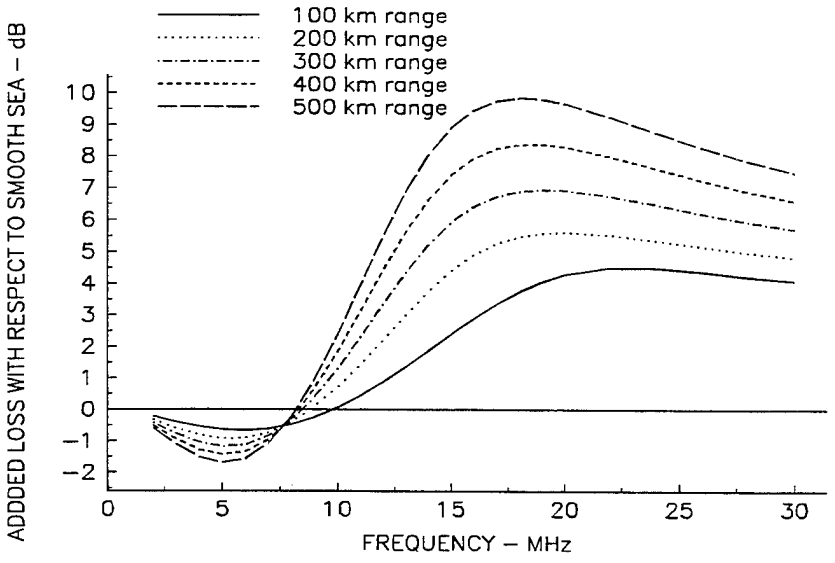

Figure 60. Added transmission loss due to sea state with 10-knot winds blowing.

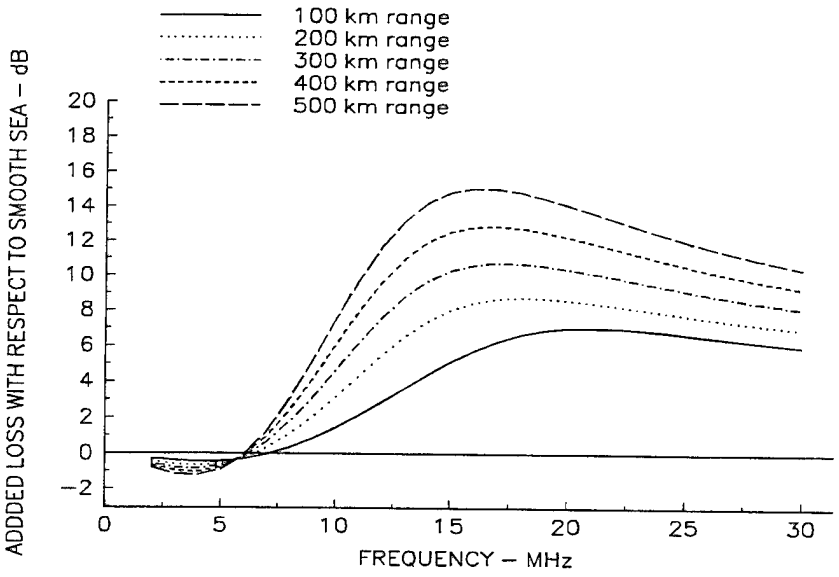

Figure 61. Added transmission loss due to sea state with 15-knot winds blowing.

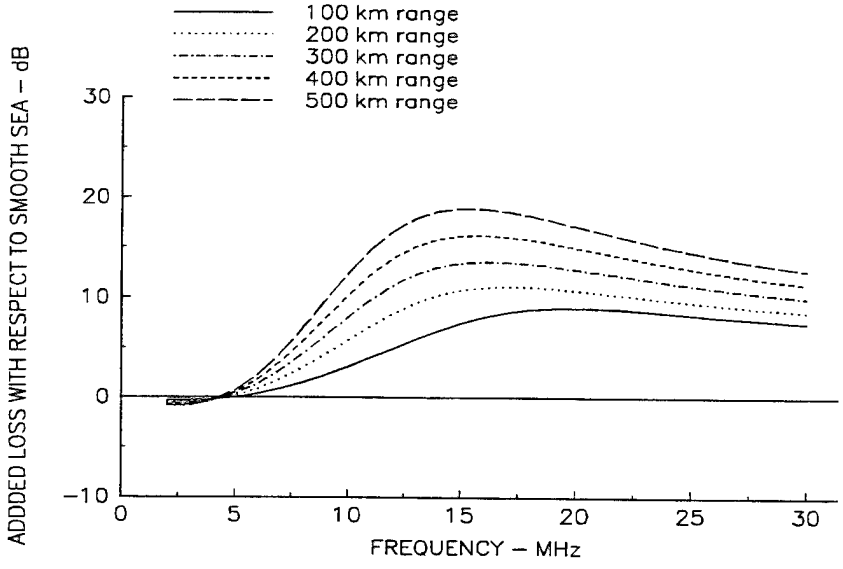

Figure 62. Added transmission loss due to sea state with 20-knot winds blowing.

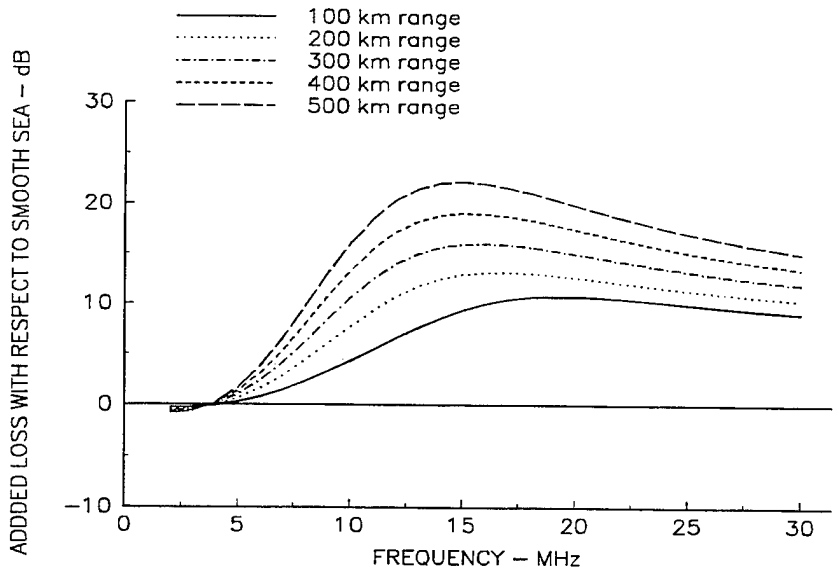

Figure 63. Added transmission loss due to sea state with 25-knot winds blowing.

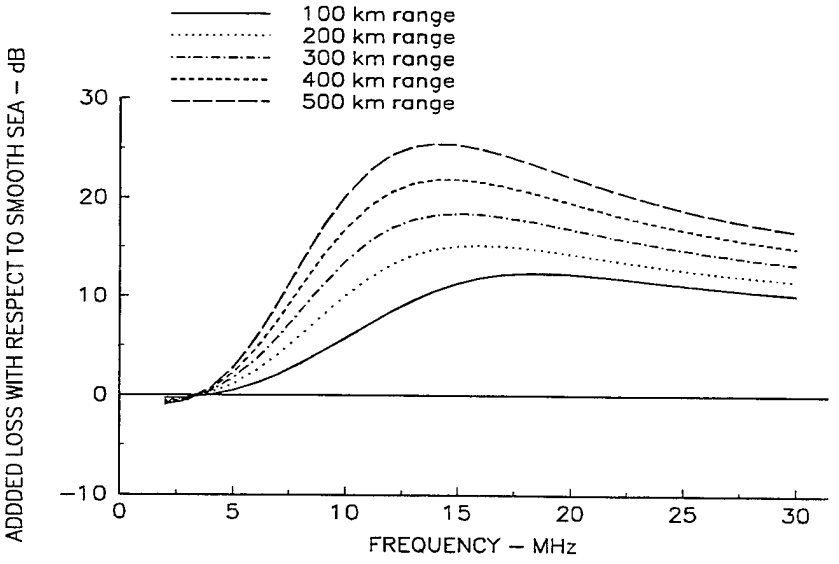

Figure 64. Added transmission loss due to sea state with 30-knot winds blowing.

REFERENCES

Barrick, D. E. 1970. "Theory of Ground-wave Propagation Across a Rough Sea at Dekameter Wavelengths," Battelle Memorial Institute (Jan).

Barrick, D. E. 1971a. "Theory of HF and VHF Propagation Across the Rough Sea, 1, the Effective Surface Impedance for a Slightly Rough Highly Conducting Medium at Grazing Incidence," *Radio Sci.* (May), vol. 6, no. 5, pp. 571-526.

Barrick, D. E. 1971b. "Theory of HF and VHF Propagation Across the Rough Sea, 2, Application to HF and VHF Propagation Above the Sea," *Radio Sci.* (May), vol. 6, no. 5, pp. 527-533.

Berry, L. A. 1978. "Users Guide to Low-frequency Radio Coverage Programs," Office of Telecommunications Report 78-247.

International Radio Consultative Committee (CCIR). 1990. "Bandwidths, Signal-to-Noise Ratios and Fading Allowances in Complete Systems; Recommendation 339-6, " *Fixed Service at Frequencies Below About 30 MHz, Recommendations of the CCIR*, 1 1990, vol. III, International Telecommunication Union, Geneva, Switzerland.

Hatfield, V. E., B. T. Bumbaca, K. K. Bailey, and G. Smith. 1987. "AMBCOM User's Guide for Programmers (Jan)," *SRI International User's Guide*, SRI International, Menlo Park, CA.

Horn, J. M. and W. E. Gustafson. 1971. "HF Shipboard Antenna System Design and Utilization Criteria," Naval Electronics Laboratory Center TR 1808 (Dec), San Diego, CA.

Millington, G. 1949. "Ground Wave Propagation Over an Inhomogeneous Smooth Earth," *Proc. IEE Part II.*, vol. 96, no. 39, pp. 53-64.

Milson, J, D. 1976. "Standard Reference Radiators for Ground Wave Field Strength Curves," *The Marconi Review* (Third Quarter), vol. XXXIX, no. 202, pp. 117-138.

Myers, J. J., C. H. Holm, and R. F. McAllister. 1969. *Handbook of Ocean and Underwater Engineering*, pp. 11.97-11.99, McGraw-Hill Book Co., New York, NY.

Olson, I, C. 1983. "HF Communication System Link Analysis," ICS-3, Integrated Communication System HF Radio Subsystem (AN/URC-109) Quick Look Technical Assessment, performed 27 April–29 June 1983, Naval Electronics Systems Command (ELEX 06) Publication 28 (Sep).

Sailors, D. B. 1995. "A Discrepancy in the International Radio Consultative Committee Report 322-3 Radio Noise Model: The Probable Cause," *Radio Sci.* (May-Jun), vol. 30, no. 3, pp. 713-728.

Slator, T. 1978. "The Elementary Dipole and Its Reflection," *The Marconi Review* (Second Quarter), vol. XLI, no. 209.

Smith, G. and V. E. Hatfield, 1987. "AMBCOM User's Guide for Engineers," SRI International User's Guide (Jan), SRI International, Menlo Park, CA.

Sprague, R. A. 1993a. "Shipboard Propagation Prediction (SPP) Program, Version 2.2," Volume 1. Operational User's Manual. NRaD TD 2459 (Mar), Naval Command, Control and Ocean Surveillance Center RDT&E Division, San Diego, CA.

Sprague, R. A. 1993b. "Shipboard Propagation Prediction (SPP) Program, Version 2.2," Volume 2. Software Documentation. NRaD TD 2459 (Mar), Naval Command, Control and Ocean Surveillance Center RDT&E Division, San Diego, CA.

Teters, L. R., J. L. Lloyd, G. W. Haydon, and D. L. Lucas. 1983. "Estimating the Performance of Telecommunication Systems Using the Ionospheric Transmission Channel—Ionospheric Communications Analysis and Predictions Program User's Manual," National Telecommunications and Information Administration Rep. 83-127.

APENDIX A
SURFACE IMPEDANCE MODEL

This appendix provides the normalized average surface impedance model for use in a surface wave propagation prediction program. The model assumes that propagation is by vertically polarized waves along the sea surface in the HF frequency range. The surface impedance model is a function of frequency in MHz and wind speed in knots. The model assumes that the sea is fully risen. This model was developed by fitting polynomials to the results of a computer program written by Barrick (1970, 1971a, 1971b) to calculate his normalized average surface impedance model using the Phillips' isotropic ocean-wave spectrum. Because the original Barrick model is slow-running and always produces the same results for a given wind speed and frequency, a numerical approximation to it provides a more suitable model, is just as accurate in its intended application, and runs much faster.

The real and imaginary parts of the Barrick model results were fit with a two-dimensional polynomial. The resulting model is represented with five coefficients representing the frequency dependence and six coefficients representing the wind speed dependence. The FOTRAN model consists of the SURFIMP main subroutine and the two function subroutines: POLY4 and POLY5.

SURFIMP

```
*************************************************************************
*                                                                       *
*     computes the normalized average surface impedance for surface wave *
*     propagation by vertically polarized waves along the sea surface in the *
*     hf region. The surface impedance is a function of frequency in    *
*     megahertz and wind speed in knots. The model assumes that the sea *
*     is fully risen. The model is based on the work of Barrick (Radio  *
*     Sci., Vol. 6, pp 517-526 and pp 527-533, 1971). This model was    *
*     developed by fitting polynomials to the results of a computer program *
*     written by Barrick to calculate the normalized average surface    *
*     impedance. As this program is slow running and always produces the *
*     same results for a given wind speed and frequency; a numerical    *
*     approximation provides a more suitable model, is just as accurate, *
*     and runs much faster. The real and imaginary parts were fit with a two *
*     dimensional polynomial. There are 5 coefficients representing frequency*
*     dependence and 6 coefficients representing wind speed dependence. *
*                                                                       *
*     approximation valid for frequencies equal to or above 0.5 MHz     *
*                                                                       *
*     programmer: David B. Sailors                                      *
*                 NCCOSC RDTE DIV D882                                  *
*                 53570 SILVERGATE AVE RM 2505                          *
*                 SAN DIEGO CA 92152-5235                               *
*                                                                       *
*     subroutines and functions called:                                 *
*                                                                       *
*                 poly4   -  represents frequency dependence            *
*                 poly5   -  represents wind speed dependence           *
*                                                                       *
*     input parameters:                                                 *
*                                                                       *
*                 wspeed  -  wind speed in knots                        *
*                 freq    -  frequency in megahertz                     *
*                                                                       *
*     output parameters:                                                *
```

```
*                                                                      *
*                zta     -  complex normalized surface impedance       *
*                ztarea  -  real part of normalized surface impedance  *
*                ztaimg  -  imaginary part of normalized surface impedance *
*                                                                      *
************************************************************************

      subroutine surfimp(wspeed,freq,zta,ztarea,ztaimg)
      complex zta
      double precision arealp(6,5), aimgpt(6,5), cons1r(6),
     * cons2r(6),cons3r(6),cons4r(6),cons5r(6),cons1i(6),cons2i(6),
     * cons3i(6),cons4i(6),cons5i(6),constr(5), consti(5),
     * fq, ws, poly4, poly5
      equivalence (cons1r(1),arealp(1,1)),(cons2r(1),arealp(1,2)),
     * (cons3r(1),arealp(1,3)),(cons4r(1),arealp(1,4)),(cons5r(1),
     * arealp(1,5)),(cons1i(1),aimgpt(1,1)),(cons2i(1),aimgpt(1,2)),
     * (cons3i(1),aimgpt(1,3)),(cons4i(1),aimgpt(1,4)),(cons5i(1),
     * aimgpt(1,5))
      data      arealp  /  1.5138795304E-03, -2.9035269627E-05,
     *  9.8470753230E-06, -1.1465006495E-06,  4.8704628386E-08,
     * -6.8598280551E-10,  9.3204460129E-04,  4.5724529351E-05,
     * -1.4853408560E-05,  1.5562815849E-06, -5.9785329142E-08,
     *  7.8187423873E-10, -3.0171989683E-05, -5.0086696745E-06,
     *  1.5319104379E-06, -1.4339766406E-07,  5.2201410304E-09,
     * -6.6013427674E-11,  5.6024417532E-07,  1.2921909357E-07,
     * -3.8169254204E-08,  3.4635970463E-09, -1.2351117284E-10,
     *  1.5359539825E-12, -3.8331223149E-09, -9.8504621437E-10,
     *  2.8701118333E-10, -2.5613639118E-11,  8.9994370604E-13,
     * -1.1034459965E-14/
      data       aimgpt / -1.5152751349E-03, -5.2295489643E-05,
     *  1.6985113142E-05, -1.5536398742E-06,  5.2085258465E-08,
     * -5.9499158176E-10, -9.3136682762E-04,  4.1733241585E-05,
     * -1.4441800774E-05,  1.0531734606E-06, -3.0792624167E-08,
     *  3.1089498268E-10,  3.0164288998E-05, -2.2740464907E-06,
     *  6.3260580842E-07, -4.1701031099E-08,  1.0580510553E-09,
     * -8.2710239596E-12, -5.6111127225E-07,  3.5699365842E-08,
     * -1.0468889356E-08,  6.9674777190E-10, -1.7754506457E-11,
```

```
     *  1.3313076944E-13,  3.8479952890E-09, -2.3736216406E-10,
     *  7.9794425158E-11, -6.3188459319E-12,  2.0311543128E-13,
     * -2.1992585943E-15/

*    initial values

     ztarea=0.0
     ztaimg=0.0

*    calculations valid for 0.5 MHz and above
     if (freq .lt. 0.5) go to 10

     ws=dble(wspeed)
     fq=dble(freq)

*    find real part of the surface impedance

*    first determine affects of wind speed
*    determines the coefficients needed for the frequency dependence

     constr(1)=poly5(cons1r,ws)
     constr(2)=poly5(cons2r,ws)
     constr(3)=poly5(cons3r,ws)
     constr(4)=poly5(cons4r,ws)
     constr(5)=poly5(cons5r,ws)
*    then find affects of frequency

     ztarea=poly4(constr,fq)

*    then find imaginary part

*    first find affects of wind speed
*    determines the coefficients needed for the frequency dependence

     consti(1)=poly5(cons1i,ws)
     consti(2)=poly5(cons2i,ws)
     consti(3)=poly5(cons3i,ws)
```

```
      consti(4)=poly5(cons4i,ws)
      consti(5)=poly5(cons5i,ws)

*     then find affects of frequency

      ztaimg=poly4(consti,fq)
*     finally determine the complex surface impedance

10    zta=cmplx(ztarea,ztaimg)
      return
      end
```

POLY4

```
************************************************************************
*     evaluates a fourth degree polynomial                             *
*                                                                      *
*     programmer  -  David B. Sailors                                  *
*                    NCCOSC RDTE DIV 542                               *
*                    53570 SILVERGATE AVE RM 2505                      *
*                    SAN DIEGO CA 92152-5235                           *
*                                                                      *
*     formal arguments                                                 *
*            const4  -   array containing the necessary 5 coefficients *
*            x       -   independent variable                          *
*                                                                      *
************************************************************************

      double precision function poly4(const4,x)
      double precision const4(5), fx, x
      fx=const4(5)
      do i=4,1,-1
      fx=fx*x + const4(i)
      end do
      poly4=fx
      end
```

POLY5

```
*************************************************************************
*     evaluates a fifth degree polynomial                               *
*                                                                       *
*     programmer  -  David B. Sailors                                   *
*                    NCCOSC RDYE DIV 542                                *
*                    53570 SILVERGATE AVE RM 2505                       *
*                    SAN DIEGO CA 92152-5235                            *
*                                                                       *
*     formal arguments                                                  *
*            const5  - array containing the necessary 6 coefficients    *
*            x       - independent variable                             *
*                                                                       *
*************************************************************************

      double precision function poly5(const5,x)
      double precision const5(6), fx, x
      fx=const5(6)
      do i=5,1,-1
      fx=fx*x + const5(i)
      end do
      poly5=fx
      end
```

APENDIX B
VERIFICATION OF THE SURFACE IMPEDANCE MODEL

The computer model presented in appendix A was compared to actual surface impedance data produced by Barrick's surface impedance model using the Phillips' isotropic ocean-wave spectrum. The model is most accurate in the frequency range at which the affects of sea roughness are most serious. Figure B-1 presents the real part of the normalized surface roughness impedance data; Figure 2 presents the imaginary part of the normalized surface roughness impedance data. Note the irregular behavior in the data for 25- and 30-knot winds blowing for frequencies greater than 12 MHz. This behavior is more serious in the imaginary part of the normalized surface roughness impedance data. Although Barrick's figures don't show this behavior as a result of being smoothed, Barrick recognized that a restriction must be placed on the validity of his model. That restriction was that the wave height be small in terms of wavelength. This can be translated to a restriction on wind speed for a particular frequency. Clearly, the 30-knot wind speed shows this limitation.

Figures B-3 through B-10 show the result of comparing the data of figures B-1 and B-2 to similar results using the computer model of appendix A. Figures B-3 and B-4 show a scatter plot of the real and imaginary parts, respectively, of the normalized surface test data versus the estimated data by the computer model. Except at the end points, the data are nearly a straight line. Figures B-5 and B-6 show a semi-log, scatter plot of the relative error of the estimated normalized surface impedance versus frequency for the real and imaginary parts, respectively. Notice the spread, particularly below 1 MHz (i.e., 10^0 MHz is 1 MHz). From 1 MHz to 5 MHz, the relative error is as large as 10%. Below 1 MHz the relative error is negative (i.e., the model predicts high) and falls to -40% at 0.1 MHz. Figures B-7 and B-8 show the relative error in percent of the estimated normalized surface impedance versus frequency at each sea state for real and imaginary parts, respectively. Again, at frequencies greater than 10 MHz, the fit is very good. Between 1 MHz and 10 MHz, the fit appears to be best for the higher wind speeds for the real part. For the imaginary part in this frequency range, just the opposite is true; the lower wind speeds are more accurate. Finally, figures B-9 and B-10 show the mean and standard deviation in the relative error in percent of the estimated normalized surface impedance versus frequency for the real and imaginary parts, respectively. Note that the mean error never gets above 10% above 1 MHz and is nearly zero above 10 MHz. The spread in error increases as the frequency decreases below 10 MHz. At 2 MHz the standard deviation is $\pm$ 5%.

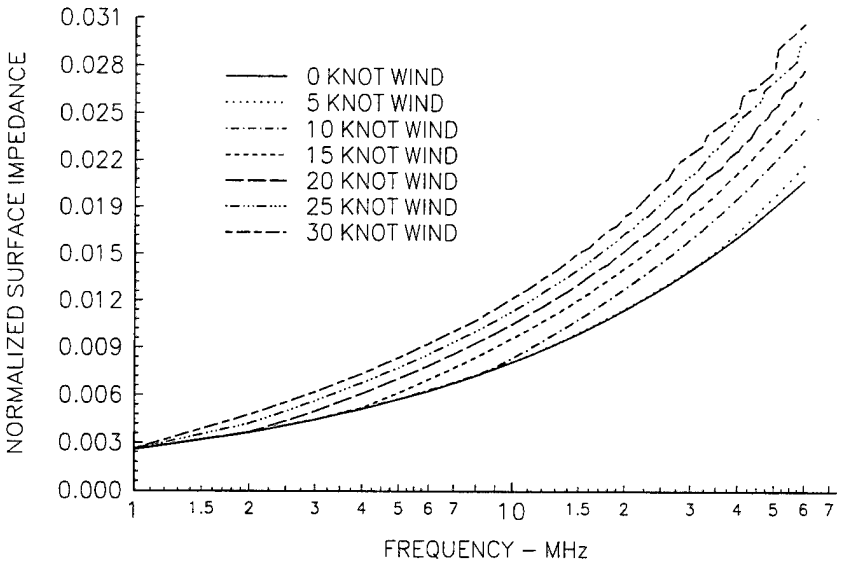

Figure B-1. Normalized surface roughness impedance data—real part.

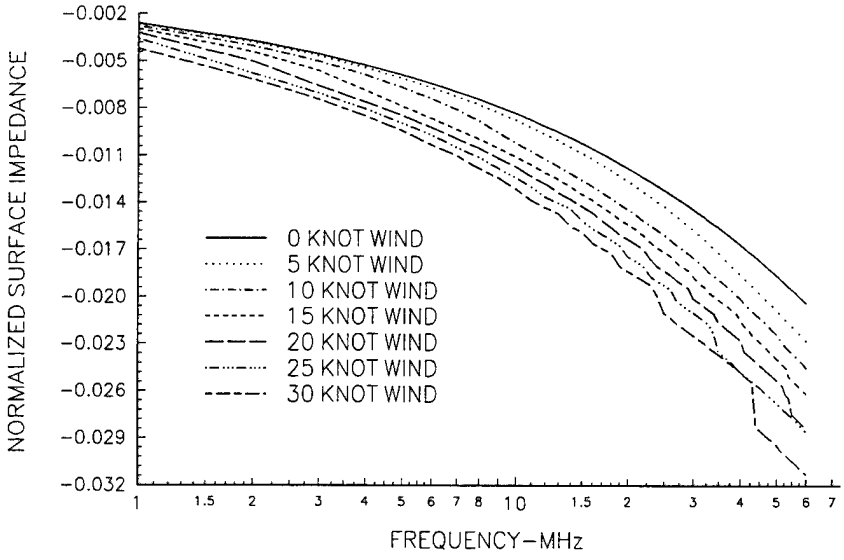

Figure B-2. Normalized surface roughness impedance data—imaginary part.

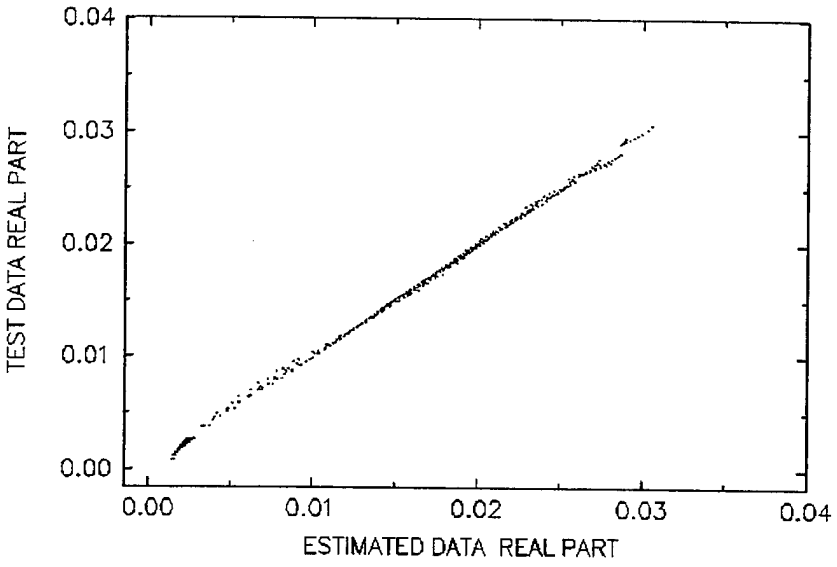

Figure B-3. Scatter plot of normalized surface impedance test data versus estimated data—real part.

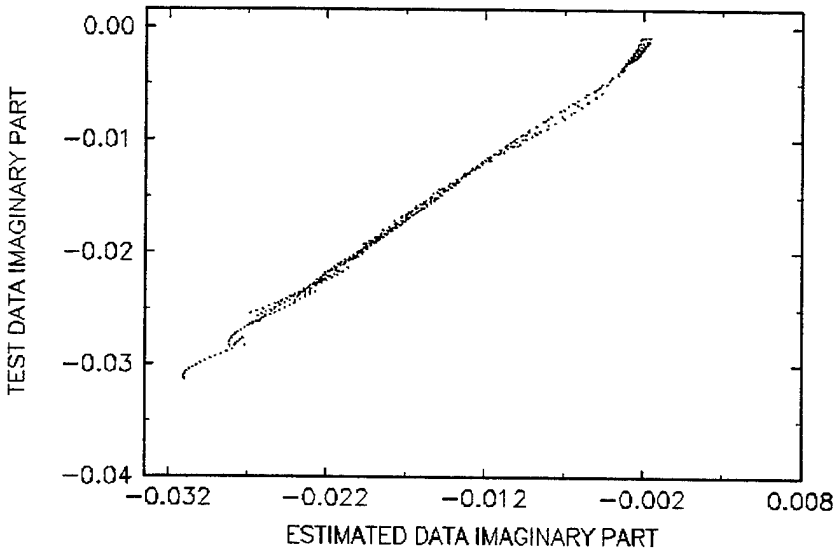

Figure B-4. Scatter plot of normalized surface impedance test data versus estimated data—imaginary part.

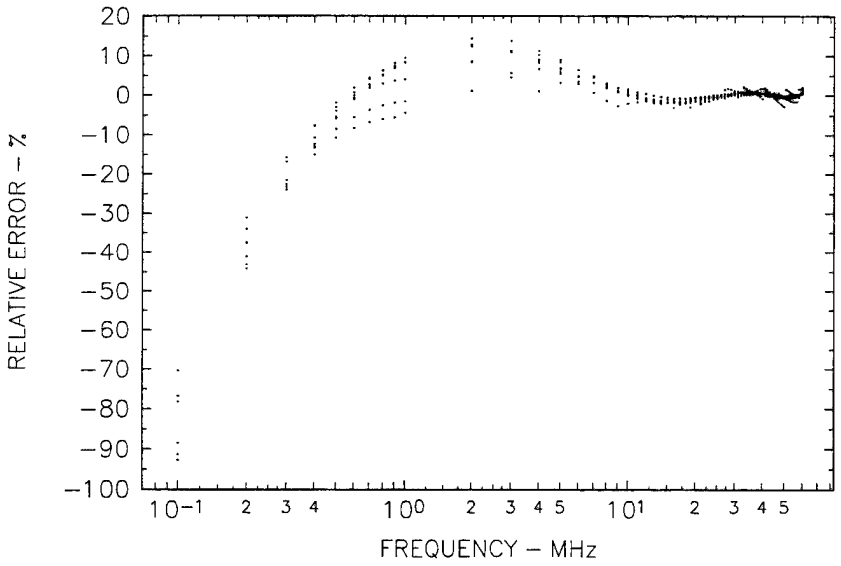

Figure B-5. Relative error in percent of the estimated normalized surface impedance versus frequency—real part.

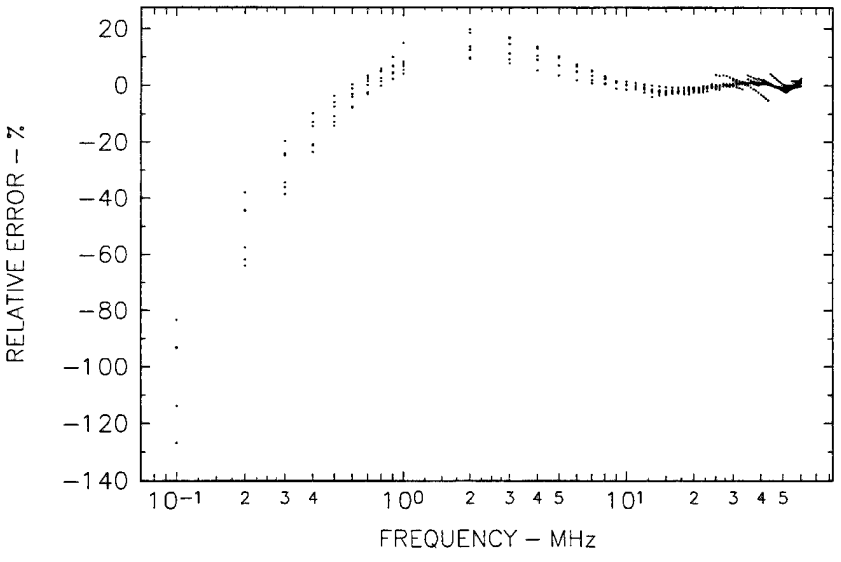

Figure B-6. Relative error in percent of the estimated normalized surface impedance versus frequency—imaginary part.

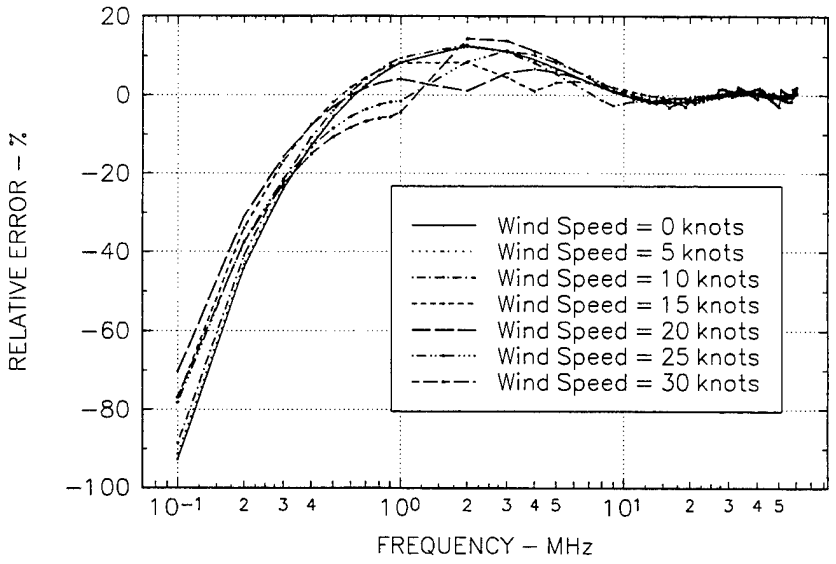

Figure B-7. Relative error in percent of the estimated normalized surface impedance versus frequency at each sea state—real part.

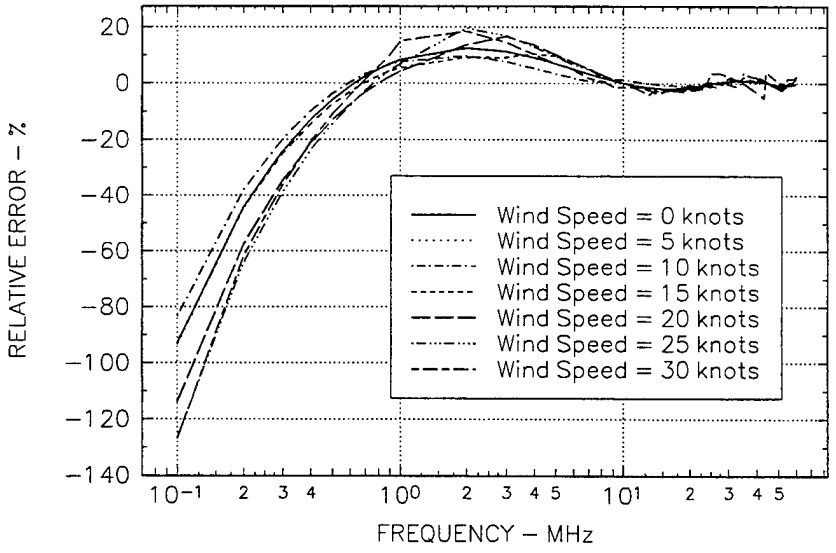

Figure B-8. Relative error in percent of the estimated normalized surface impedance versus frequency at each sea stare—imaginary part.

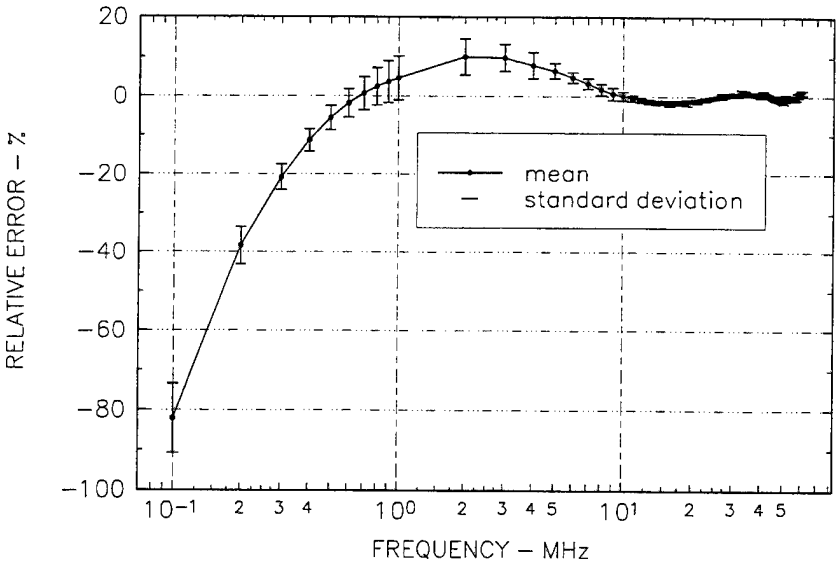

Figure B-9. Mean and standard deviation in the relative error in percent of the estimated normalized surface impedance versus frequency—real part.

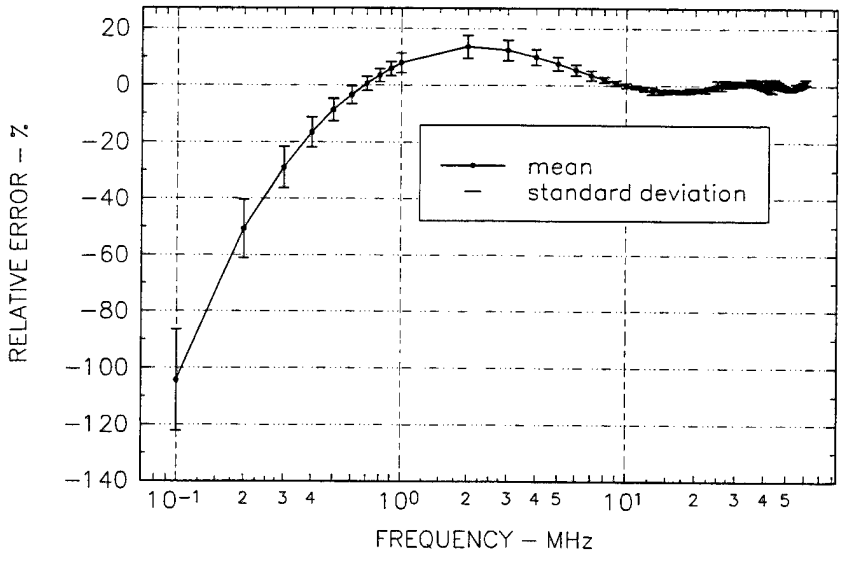

Figure B-10. Mean and standard deviation in the relative error in percent of the estimated normalized surface impedance versus frequency—imaginary part.

REPORT DOCUMENTATION PAGE

Form Approved
OMB No. 0704-0188

1. AGENCY USE ONLY *(Leave blank)*	2. REPORT DATE	3. REPORT TYPE AND DATES COVERED
	August 1997	Final: March–May 1996 May–June 1997

4. TITLE AND SUBTITLE
EXCESS SYSTEM POWER AVAILABLE FOR SHORT-RANGE HIGH-FREQUENCY COMMUNICATIONS SYSTEMS

5. FUNDING NUMBERS
PE: 0204163N
AN: DN305541
WU CM-76

6. AUTHOR(S)
D. B. Sailors

7. PERFORMING ORGANIZATION NAME(S) AND ADDRESS(ES)
Naval Command, Control and Ocean Surveillance Center (NCCOSC)
RDT&E Division (NRaD)
San Diego, CA 92152–5001

8. PERFORMING ORGANIZATION REPORT NUMBER

9. SPONSORING/MONITORING AGENCY NAME(S) AND ADDRESS(ES)
Space and Naval Warfare Systems Command
PMW–146
Washinton, DC 20363–5100

10. SPONSORING/MONITORING AGENCY REPORT NUMBER
TD 2978

11. SUPPLEMENTARY NOTES

12a. DISTRIBUTION/AVAILABILITY STATEMENT
Approved for public release; distribution is unlimited.

12b. DISTRIBUTION CODE

13. ABSTRACT *(Maximum 200 words)*

This report presents the result of a surface-wave propagation study to determine the excess available transmission power over sea to a short-range (i.e., less than 500 km), high-frequency (HF) communication system.

14. SUBJECT TERMS
Mission Area: Communications
radio communication systems — high frequency
short-range communications — surface-wave propagation

15. NUMBER OF PAGES
83

16. PRICE CODE

17. SECURITY CLASSIFICATION OF REPORT	18. SECURITY CLASSIFICATION OF THIS PAGE	19. SECURITY CLASSIFICATION OF ABSTRACT	20. LIMITATION OF ABSTRACT
UNCLASSIFIED	UNCLASSIFIED	UNCLASSIFIED	SAME AS REPORT

21a. NAME OF RESPONSIBLE INDIVIDUAL	21b. TELEPHONE *(include Area Code)*	21c. OFFICE SYMBOL
D. B. Sailors	(619) 553-3063 e-mail: sailors@nosc.mil	Code D882

INITIAL DISTRIBUTION

Code D0012	Patent Counsel	(1)
Code D0271	Archive/Stock	(6)
Code D0274	Library	(2)
Code D027	M. E. Cathcart	(1)
Code D0271	D. Richter	(1)
Code D451	R. Hollandsworth	(1)
Code D623	C. Moussa	(1)
Code D73J	J. Audia	(1)
Code D772	B. Satterlee	(1)
Code D824	H. Guyader	(1)
Code D827	R. Merk	(1)
Code D832	G. Crane	(1)
Code D8405	G. Clapp	(1)
Code D8405	C. Fuzak	(1)
Code D841	R. Axford	(1)
Code D846	T. Danielson	(10)
Code D846	L. Pinck	(1)
Code D846	J. Ramos	(1)
Code D846	C. Liou	(1)
Code D846	H. Wiesenfarth	(1)
Code D846	P. Francis	(1)
Code D846	S. Valvonis	(1)
Code D8505	D. Tam	(1)
Code D851	P. Li	(1)
Code D855	R. North	(1)
Code D88	J. Richter	(1)
Code D8805	D. Gingras	(1)
Code D882	J. Ferguson	(2)
Code D882	D. B. Sailors	(15)
Code D882	R. Sprague	(1)

Defense Technical Information Center
Fort Belvoir, VA 22060–6218 (4)

NCCOSC Washington Liaison Office
Arlington, VA 22245–5200

Center for Naval Analyses
Alexandria, VA 22302–0268

Navy Acquisition, Research and Development
Information Center (NARDIC)
Arlington, VA 22244–5114

GIDEP Operations Center
Corona, CA 91718–8000

Space and Naval Warfare Systems Command
Arlington, VA 22245–5200 (2)

Space and Naval Warfare Systems Command
San Diego, CA 92110–3127 (5)

Office of Naval Research
Arlington, VA 22217–5660 (4)

Navy Research Laboratory
Washington, DC 20375–5000 (2)

USA CECOM
Ft. Monmouth, NJ 07703–5000 (2)

Naval Surface Warfare Center
Coastal Systems Station
Dahlgren Division
Panama City, FL 32407–7001 (2)

Irv Olson
Paso Robles, CA 93446–9357

USAF RADC (2)

Naval Coastal System Station (2)

Chief of Naval Operations
Washington, DC 20350–2000 (2)

DOD Joint Spectrum Center
Annapolis, MD 21402–5064 (3)

Naval Electromagnetic Spectrum Center
Washington, DC 20394–5460